University of South-Eastern Norway

www.usn.no

FMH606 Master's Thesis 2022

Master of Science, Energy and Environmental Technology

Modelling heat treated lignocellulosic material as substrate in anaerobic digestion

Alireza Rasti

Faculty of Technology, Natural sciences and Maritime Sciences
Campus Porsgrunn

University of South-Eastern Norway

www.usn.no

Course: FMH606 Master's Thesis, 2022

Title: Modelling heat treated lignocellulosic material as substrate in anaerobic digestion

Number of pages: 66

Keywords: Anaerobic digestion, Pyrolysis, Aqueous pyrolysis liquid, Syngas, ADM1, Lignocellulosic biomass

Student: Alireza Rasti

Supervisor: Wenche Hennie Bergland

External partner: Gudny Øyre Flatabø at Scanship AS

Availability: Open

University of South-Eastern Norway

www.usn.no

Summary:

Clean energy technology is quickly establishing itself as a major new source of investment and job development, as well as a vibrant sector for international competition. Anaerobic digestion of biomass requires less capital and per unit production cost than other renewable energy sources. Biomass can be utilized to substitute a reliable and renewable energy source for fossil fuels and can be found in a wide range of materials, including wood, sawdust, straw, seed waste, manure, paper trash, household waste, wastewater, and so on. Anaerobic digestion is a collection of biological processes that use a wide population of bacteria to break down organic materials into biogas, primarily methane, and a mixture of solids and liquid effluents. Lignocellulosic biomass by having cellulose and hemicellulose is appropriate for Anaerobic digestion process. Using thermochemical or biochemical conversion processes, lignocellulosic biomass can be converted into energy or energy carriers. Pyrolysis is one of the most cost-effective and environmentally friendly technologies for biomass conversion and converts dry biomass into charcoal, syngas, bio-oil, and aqueous pyrolysis liquid (APL). Feedstock, particle size, heating rate, temperature, and other parameters all influence yields and composition.

In this work, a study of integrating of anaerobic digestion and pyrolysis process using Anaerobic Digestion Model No. 1 (ADM1) as base model and modified to simulate and evaluate the changes in methane production rate by coupling pyrolysis products of APL, and syngas to AD has been done. Different time steps of basic condition of modelling and simulation of full-scale operation of Lindum's reactors with full capacity at time step zero with 80% volume of reactors, time step one by adding APL as co-substrate, time step two by adding syngas as co-substrate, and time step three by adding combination of syngas and APL as co-substrate, were investigated. At first, by some adjustment of time step zero by increasing concentration of alkalinity, ammonium, and inorganic cation slightly, the percentage of methane produced increased to some degree. In time step one, by coupling AD reactor to pyrolysis process with adding APL as co-substrate led to the about 0.31 percent increases of methane percentage produced in comparison to time step zero. In time step two, adding all 100 % of syngas as co-substrate to AD led to 9% reduction in methane percentage produced, and by reducing the amount of coupled syngas to 10% the methane percentage produced becomes more or less similar to time step zero. With using hydrogen-rich syngas with 86% H2, 7% CO, and 7% CO2 in ADM1 the methane percentage produced increases by 4% in comparison to time step zero. In time step three the combination of syngas and APL added to the AD reactor as co-substrate. Adding 10% syngas of time step two along with APL causes 10% reduction in methane percentage produced. While, by increasing the addition of syngas from ten percent to 100% of produced syngas to the AD reactor the methane percentage produced increases by 2% in comparison to time step zero.

Preface

This thesis was completed as a fulfillment of a partial requirement to achieve a master's degree in Energy and Environmental Technology at the University of South-Eastern Norway.

I wish to express my most sincere gratitude to my main supervisor Assoc. Prof. Wenche Hennie Bergland for her guidance, time, support, and help throughout the thesis. Also, I would like to thank our external partner Gudny Øyre Flatabø for her guidance.

I dedicate my thesis work to the beautiful and pure soul of my brother, Hamidreza, whose love is in every single cell of my heart and his memory is in my mind till my last breath. There is always a special place in my heart for you.

Porsgrunn, 16.05.2022

Alireza Rasti

Contents

List of tables

List of figures

Nomenclature

Abberviation	Explanations
AD	Anaerobic Digestion
ADM1	Anaerobic Digestion Model No. 1
APL	Aqueous Pyrolysis Liquid
HS	Hydrolysed Sludge
IWA	International Water Association
LCFA	Long Chain Fatty Acid
OL	Organic Load
COD	Chemical Oxygen Demand
sCOD	Soluble COD
TAN	Total Ammonium Nitrogen
tCOD	Total chemical oxygen demand
VFA	Volatile fatty acids
VS	Volatile solids
AA	Amino acids
HMF	5-hydrooxymethylfurfural
pH	Potential of hydrogen

Chemical compound	Explanations
CH4	Methane
CO	Carbon Monoxide
CO2	Carbon dioxide
H2O	Water
H2	Hydrogen gas
NH4	Ammonium

Symbol	Explanations	Unit
X_ch	Particulate Carbohydrate	[kg COD/m3]
X_I	Particulate Inert	[kg COD/m³]
X_li	Particulate Lipids	[kg COD/m³]
X_pr	Particulate Protein	[kg COD/m³]
X_C	Particulate Composite	[kg COD/m³]
S_IC	Alkalinity	[mol/L]
S_IN	Ammonium	[mol/L]

1 Introduction

Because of the rise in global energy consumption dependence on fossil fuels, which accounts for 80% of total required energy, there have significant energy crises in recent years, which are inextricably linked to massively escalating environmental pollution and fossil fuel resource scarcity [1]. The technology of clean energy is rapidly emerging as a major new source of investment and job creation, as well as a vibrant field for international effort and rivalry [2]. Among the different alternative energy sources now accessible such as solar, hydro, wind, biomass, and geothermal, biomass-based renewable energy is one of the most efficient and effective. In comparison to other renewable energy sources, anaerobic digestion of biomass demands lower capital investment and per unit production cost. [1] Biomass is a renewable resource found in a wide range of materials, including wood, sawdust, straw, seed waste, manure, paper trash, household waste, wastewater, and so on. Biomass resources have long been used, and their use is becoming more important due to their economic potential, as there are significant annual volumes of agricultural production whose by-products could be used as an energy source, and are being presented as "energy crops" for this aim [3]. It can be used to replace fossil fuels with a dependable and renewable local energy source. The annual production of biomass is expected to be 146 billion metric tons, with the majority of this coming from natural plant growth. Biomass fuel is a renewable energy source that will become more prominent as national energy policy and strategy emphasize renewables and conservation [4]. Biomass-to-energy is a sustainable option for reducing greenhouse-gas emissions in the atmosphere, providing that secondary and tertiary biomass are used instead of fossil fuels. In developing and rising economies, agricultural and forest-based sectors create a significant amount of biomass residue and waste that may potentially be used for production of energy [5]. Biomass is converted to energy utilizing two main process technologies: thermochemical and biochemical/biological. There are four process alternatives for thermo-chemical conversion: combustion, pyrolysis, gasification, and liquefaction. Digestion (the production of bio-gas, a mixture primarily of methane and carbon dioxide) and fermentation are two bio-chemical conversion processes (production of ethanol). Figure 1.1 shows the Main processes, intermediate energy carriers and final energy products from the thermo-chemical conversion of biomass [6].

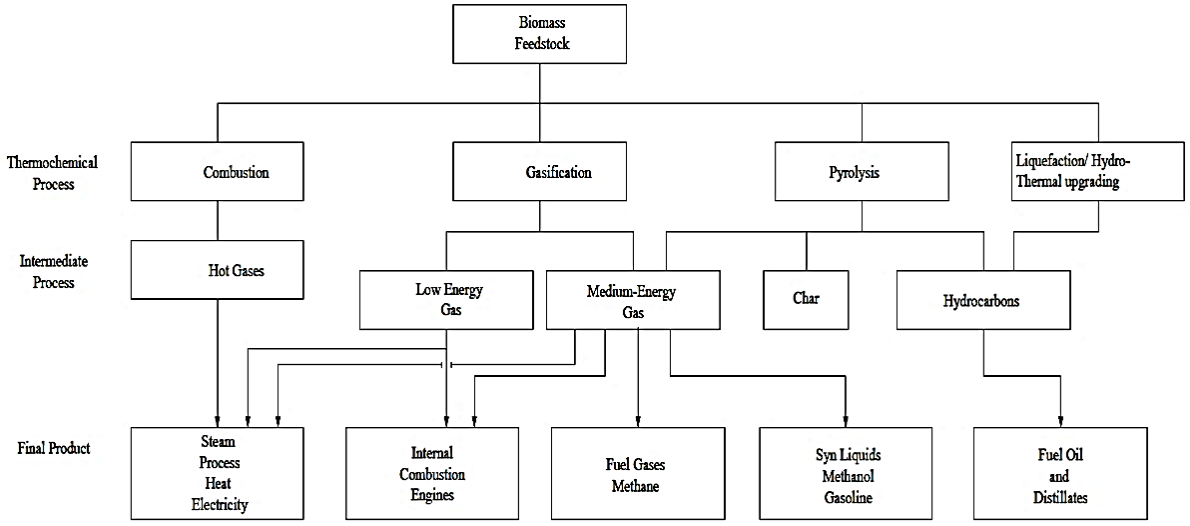

Figure 1.1: Thermo-chemical conversion of biomass: main processes, intermediate energy carriers, and final energy product [6].

Pyrolysis is the process of converting biomass into liquids (bio-oil or bio-crude), solids, and gases [6], which is also known as thermolysis, and is an irreversible thermochemical treatment of complex solid or fluid chemical compounds at elevated temperatures in an inert or oxygen-free atmosphere, with a rate of pyrolysis that is temperature dependent and increases with temperature. Pyrolysis causes molecules to be stretched and shook to the point where they start breaking down into smaller molecules due to extremely high temperatures. Pyrolysis is frequently the first step in other processes involving partial or complete oxidation of the treated material, such as gasification and combustion. Pyrolysis is derived from two Ancient Greek words pyro (πυρο) meaning fire and lysis (λύσις) meaning separating (or solution), hence pyrolysis refers to the separation of materials by fire or heat [7]. Pyrolysis technology was utilized to make charcoal more than 5500 years ago in Southern Europe and the Middle East. Pyrolysis technique can produce biofuels with high fuel-to-feed ratios. As a result, pyrolysis has gotten increased attention in recent decades as an effective technique of converting biomass into biofuel. The ultimate goal of this technique is to produce high-value bio-oil that can compete with non-renewable fossil fuels and even replace them. Figure 1.2 shows pyrolysis energy products [8].

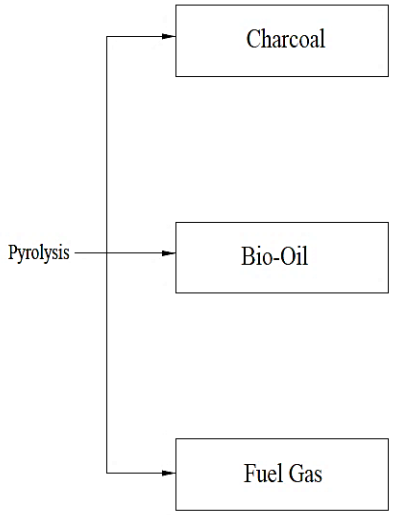

Figure 1.2: Energy products from pyrolysis [8].

All plants and plant-derived materials, including agricultural crops and trees, timber and wood leftovers, municipal residues, and other residue materials, are classified as lignocellulosic biomass [9]. Plant cell walls are made up primarily of lignocellulose. cellulose, hemicellulose, and lignin account for the majority of plant biomass, with smaller amounts of pectin, protein, extractives (soluble nonstructural elements such nonstructural sugars, nitrogenous material, chlorophyll, and waxes), and ash. The content of these elements varies depending on the plant species. Hardwood, for example, contains more cellulose, whereas wheat straw and leaves have more hemicellulose. Table 1.1 gives an overview of Contents of cellulose, hemicellulose, and legin in agricultural residues and wastes [10].

Table 1.1: Contents of cellulose, hemicellulose, and legin in agricultural residues and wastes [10].

Lingocellulosic material	Cellulose (%)	Hemicellulose (%)	Lingin (%)
Harwood stems	40-55	24-40	18-25
Softwood stems	45-50	25-35	25-35
Nut shells	25-35	25-35	30-40
Corn cobs	45	35	15
Grasses	25-40	35-50	30-Oct
Paper	85-99	0	0-15
Wheat straw	30	50	15
Sorted refuse	60	20	20
Leaves	15-20	80-85	0
Cotton seed hairs	80-95	20-May	0
Newspapers	40-55	25-40	18-30

Waste papers from chemical pulps	60-70	20-Oct	10-May
Primary wastewater solids	15-Aug		
Solid cattle manure	1.6-4.7	1.4-3.3	2.7-5.7
Coastal bermudagrass	25	35.7	6.4
Switchgrass	45	31.4	12
Swine waste	6	28	NA

The three main components of lignocellulosic biomass are cellulose, hemicellulose, and lignin [11]. Lignin protects cellulose and hemicellulose and serves as a barrier to their decomposition throughout anaerobic digestion. A high concentration of lignin is also known to reduce biomethane potential. Anaerobic digestion is hampered by slow degradation/decomposition under anaerobic conditions (AD). As a result, it must be pretreated before being used in anaerobic digestion (AD) [12]. For treating lignocellulosic biomass, pyrolysis is a widely accepted method because it produces high-value products including syngas, biochar, and bio-oil, all of which can be utilized for a variety of purposes [13]. Aqueous pyrolysis liquid (APL) is a high-COD byproduct of lignocellulosic biomass pyrolysis that can be used as a feed for anaerobic digestion (AD) [14].

Hence, this thesis would focus on evaluating model using sludge/food waste fed full scale reactors at Lindum fed syngas from pyrolysis and Aqueous Pyrolysis Liquid (APL) as co-substrates in a continuous AD reactor. Here a range of standard model parameters with some adjustment based on the analysis to see how much the concentration of CH4, and PH will be changed.

2 Theory

The anaerobic digestion process, pyrolysis and its byproducts, as well as the content of APL and the inhibition caused by APL constituents during the AD process, are all covered in this chapter.

2.1 Anaerobic Digestion (AD)

Anaerobic digestion is a set of biological processes that break down organic materials into biogas, predominantly methane, and a mix of solids and liquid effluents using a diverse population of bacteria. It develops when there isn't any free oxygen available (anoxic conditions) [15].

There are several types of anaerobic digestion methods, each with its own organic loading rates and internal mixing parameters. Up flow anaerobic sludge blanket (UASB) reactors can treat moderate organic loading rates (5–10 kg COD/m3/day), whereas expanded granular sludge blanket reactors may handle up to 25 kg COD/m3/day due to effluent recycling. The hydraulic retention time for wastewater treatment ranges from a few hours to many weeks for waste activated sludge (WAS) treatment [16]. According to the dry matter of the initial substrate the technology of AD can be characterized as follows: Wet digestion, in which the substrate's dry matter content must be less than 10%; dry digestion, whereby the substrate's dry matter content must be greater than 20%; and dry matter digestion intermediate, known as semi-dry [17].

To break down complex organic matter into soluble monomers such as amino acids, fatty acids, simple sugars, and glycerols, the process is strongly reliant on the mutual and syntrophic interaction of a consortium of microorganisms. Understanding these biological processes and the chemical reactions that go along with them is critical for optimizing AD processes [18].

2.1.1 Steps of Anaerobic Digestion

The overall anaerobic digestion of a waste involves three main steps: hydrolysis, acidogenesis (also known as fermentation or anaerobic digestion), and methanogenesis. Some of the VFAs created during acidogenesis go through an intermediate process called acetogenesis [19]. Figure 2.1 shows the fate of solids through hydrolysis, volatile fatty acids (VFAs), and hydrogen generation to methane.

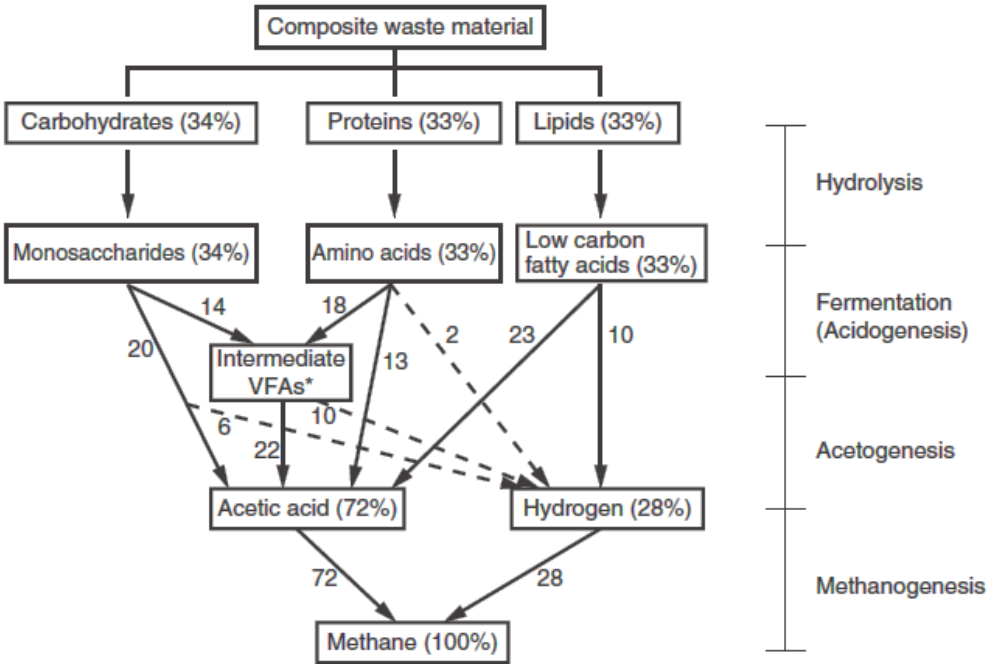

Figure 2.1: The fate of biodegradable COD in waste solids processing under anaerobic conditions [19].

- **Steps one. Hydrolysis**

The breakage of chemical bonds by the addition of water is referred to as hydrolysis in chemistry. Cations and anions react with water molecules, causing breakage of H–O bonds and changing the pH in the process. In the AD process, hydrolysis is the initial stage. It's a slow stage that can limit the overall digestion process, especially when solid waste substrates are utilized; the reaction for this step is described in Equation (2.1) which with the addition of water (H2O), cellulose (C6H10O5) is hydrolyzed, yielding glucose (C6H12O6) as the major product and and giving off H2.

$$(C_6H_{12}O_6)n + n\,H_2O \rightarrow n\,C_6H_{12}O_6 + n\,H_2 \qquad (2.1)$$

Insoluble organic molecules in the substrate, such as cellulose, are transformed to soluble organic compounds at this stage. Organics that are insoluble in H2O are solubilized by anaerobes, allowing chemical bonds to be broken and soluble substances to be formed, which bacteria cells can use. Some of the products produced during the hydrolysis step (such as H2 and CH3COO) can be utilised directly by methanogens, whereas others, which are made up of bigger molecules, are transformed to smaller molecules like acetic acid CH3COOH which are also known as ethanoic acid). Fermentative microorganisms utilize the CH3COO and H2 generated in the hydrolysis stage to make higher chain organic compounds like VFAs (volatile fatty acids) in the next stage [18].

- **Steps two. Acidogenesis**

Acidogenic bacteria can produce intermediate volatile fatty acids (VFAs) and other compounds by absorbing the products of hydrolysis through their cell membranes. VFAs contain organic acids that include acetates and larger organic acids such as propionate and butyrate, and smaller levels of ethanol and lactate may be present. Acidogenesis, in contrast to the other stages of

anaerobic digestion, is thought to progress faster than the others, with acidogenic bacteria having a regeneration time of less than 36 hours. It's worth noting that, while the formation of VFAs produces direct precursors for the final stage of methanogenesis, VFA acidification has been frequently documented as a cause of digester failure. Degradation of amino acids also produces ammonia which at high concentrations is anaerobic digestion inhibitor [20].

The reaction sequence that describes the acidogenic stage of AD is shown in Equations (2.2), (2.3), (2.4) [18].

$$C_6H_{12}O_6 \leftrightarrow 2\ CH_3CH_2OH + 2CO_2 \quad (2.2)$$

$$C_6H_{12}O_6 + 2H_2 \ \leftrightarrow 2CH_3CH_2COOH + 2H_2O \quad (2.3)$$

$$C_6H_{12}O_6 \rightarrow 3\ CH_3COOH \quad (2.4)$$

- **Steps three. Acetogenesis**

Acetogenesis is the conversion of higher VFAs and also other intermediates to acetate, including the production of hydrogen as the waste product [20]. Dehydrogenation is another name for this stage. This is because the H2 gas produced inhibits the metabolism of acetogenic bacteria. The H2 gas, on the other hand, can be ingested by CH4-producing bacteria, allowing them to act as hydrogen-scavenging bacteria, transforming some of the bacteria to CH4 [18]. Acetogenic bacteria break down the acidogenesis products into hydrogen, carbon dioxide, and acetic acid. Acetogenic bacteria are hydrogen-sensitive and prefer low hydrogen pressure to convert all intermediate acids to acetic acids [19]. The reaction sequence that describes the acetogenic stage of AD is shown in Equations (2.5), (2.6), (2.7) [18].

$$CH_3CH_2COO^- + 3\ H_2O \ \leftrightarrow CH_3COO^- + H^+HCO_3^- + 3\ H_2 \quad (2.5)$$

$$C_6H_{12}O_6 + 2\ H_2O \ \leftrightarrow 2\ CH_3COOH + 2\ CO_2 + 4\ H_2 \quad (2.6)$$

$$CH_3CH_2OH + 2\ H_2O \ \leftrightarrow CH_3COO^- + 3\ H_2 + H^+ \quad (2.7)$$

- **Steps four. Methanogenesis**

Methanogenesis is the final step in AD process where methanogenic bacteria utilize available intermediates to create methane. They CH3COOH and H2 into CO2 and CH4 [18]. Methanogenic bacteria are obligate anaerobic archaea; 99 percent of Methanococcus voltae and Methanococcus vannielli cells were destroyed after ten hours of being exposed to oxygen, demonstrating their extreme sensitivity to oxygen and they demand a higher pH in comparison to previous stages. At the same time, methanogens seem to have a substantially longer regeneration period in anaerobic digestion than other microorganisms, ranging from 5 to 16 days [20].

Because the stages preceding the methanogenic stage solely convert organic matter from one form to another, the anaerobic process in the methanogenic stage reduces organic pollution load in terms of chemical oxygen demand (COD) or biochemical oxygen demand (BOD), efficient methanogenesis is commonly performed in order to ensure effective removal of carbonaceous pollution [18].

The reaction sequence that describes the methanogenic stage of AD is shown in Equations (2.8), (2.9), (2.10) [18].

$$CH_3COOH \ \rightarrow CH_4 + CO_2 \quad (2.8)$$

$$CO_2 + 4\,H_2 \rightarrow CH_4 + 2\,H_2O \quad (2.9)$$

$$2\,CH_3CH_2OH + CO_2 \rightarrow CH_4 + 2\,CH_3COOH \quad (2.10)$$

2.1.2 Parameters affecting anaerobic digestion

In order to improve the anaerobic digestion process, various critical process parameters, growth kinetics, and environmental conditions must be managed. The following subsections describe the most important parameters.

- **Alkalinity and pH**

The pH level should be between 6.8 and 7.2 for AD process to perform properly. For optimal pH management, there must be sufficient alkalinity. Alkalinity acts as a buffer, slowing down the rate at which pH changes. pH has an effect on enzyme activity as well as digestion performance. Acid-forming bacteria have adequate enzymatic activity above pH 5.0, whereas methane-forming bacteria do not have acceptable enzymatic activity below pH 6.2. The pH range of 6.8 to 7.2 is ideal for the majority of anaerobic bacteria, including methane-forming bacteria [21]. Alkalinity is produced in wastewater by calcium, magnesium, sodium, potassium, and ammonium hydroxides and carbonates [22]. The total alkalinity of a well-established digester ranges between 2000 and 5000 mg/L, and it is proportional to the solids feed concentration [19].

- **Temperature**

Temperature is important in anaerobic digestion because it sets up microbial ecosystems and, as a result, controls the process's stability [23].

The ideal temperature for biogas production in a mesophilic digester is 35°C. Each 10°C reduction in the mesophilic range reduces the activity and growth rate of bacteria by 50%. When temperatures drop below 20°C, biogas production declines and eventually stops around 10°C. The digesting process takes less time when the temperature is raised to 37°C. The rate of biogas production reduces as the temperature rises [24].

- **Solids and Hydraulic Retention Time**

The average time solids and liquids are kept in the digesting process is called the solids and hydraulic retention times (SRT and HRT). These factors are directly related to anaerobic reactions (hydrolysis, fermentation, and methanogenesis) and anaerobic reactor size. Each anaerobic digestion reaction requires a minimum SRT to perform, and the digestion process will fail if the design SRT is smaller. Solids and hydraulic retention times are the same in a completely mixed reactor with no recycle. SRT values for high-rate digestion range from 10 to 20 days [19].

- **Toxic Substances**

Toxicants can hinder anaerobic digestion, causing irritation or failure [25]. Toxicity can be caused by a number of inorganic and organic wastes in anaerobic digesters. In primary clarifiers, many harmful wastes are eliminated and transported straight to the anaerobic digester. In primary sludge, heavy metals can precipitate as hydroxides, while organic

substances like oils and chloroform are eliminated in primary scum and sludge, respectively. Wastes that are harmful to anaerobic digesters are frequently found in industrial wastewaters. Table 2.1 shows anaerobic digesters' list of toxic inorganic and organic wastes.

Table 2.1: Inorganic and organic toxic wastes to anaerobic digesters [21].

No.	List of inorganic and organic toxic wastes to anaerobic digesters
1	Alcohols (isopropanol)
2	Alkaline cations (Ca^{2+}, Mg^{2+}, K^{+}, and Na^{+})
3	Alternate electron acceptors, nitrate (NO^{-}_{3}) and sulfate (SO_4^{2-})
4	Ammonia
5	Benzene ring compounds
6	Cell bursting agent (lauryl sulfate)
7	Chemical inhibitors used as food preservatives
8	Chlorinated hydrocarbons
9	Cyanide
10	Detergents and disinfectants
11	Feedback inhibition
12	Food preservatives
13	Formaldehyde
14	Heavy metals
15	Hydrogen sulfide
16	Organic-nitrogen compounds (acrylonitrile)
17	Oxygen
18	Pharmaceuticals (monensin)
19	Solvents
20	Volatile acids and long-chain fatty acids

In an anaerobic digester, toxicity can be acute or chronic. Acute toxicity occurs when an unacclimatized population of bacteria is exposed to a relatively high concentration of a toxic waste in a short period of time. Chronic toxicity occurs when an unacclimatized population of bacteria is exposed to a toxic waste over a lengthy period of time. Toxicity indicators can emerge quickly or slowly in an anaerobic digester, depending on the type of toxicity and the concentration of hazardous waste. The disappearance of hydrogen, the disappearance of methane, declines in alkalinity and pH, and an increase in volatile acid concentration are all indicators of toxicity. There are numerous and diverse wastes that are harmful to anaerobic digesters. Ammonia, hydrogen sulfide, and heavy metals are among the three most widely discussed types of toxicity [21].

- **Carbon and Nutrients Availability**

Carbon, nitrogen, phosphorus, and sulfur are essential nutrients for the anaerobic digestion process organism's survival and growth. Different micronutrients/microelements (trace elements) are also required by anaerobic process bacteria, such as iron, nickel, cobalt, selenium, molybdenum, or tungsten. Inadequate amounts of essential minerals and trace elements can cause anaerobic digestion to be inhibited and unstable. To maintain optimum methanogenic activity, liquid phase nitrogen, phosphorus, and sulphur concentrations should be in the range of 50, 10 and 5 mg/l, respectively. Furthermore, iron, cobalt, nickel, and zinc levels should be 0.02, 0.004, 0.003, and 0.02 mg/g acetate produced, respectively [19].

- **Organic Loading Rate (OLR)**

The amount of organic dry matter that can be fed into the digester per unit volume of its capacity per day is known as the Organic Loading Rate (OLR). The mass of volatile solids added per day per unit volume of digester capacity is commonly used to calculate it. Although the first approach is preferable, another way to calculate it is the amount of volatile solids fed to the digester each day per mass of volatile solids in the digester [19].

The loading rate of the digester is a critical operational component because if it is too high, valuable methane former can wash out of the system. Furthermore, hazardous compounds such as ammonia can build up and disrupt the process. On the other hand, with low loading rate, less organic materials are destroyed and less biogas is produced. Furthermore, larger, less cost-effective digesters will necessitate greater temperatures. As a result, the optimal loading rate should be a balance between maximizing biogas production while maintaining a reasonable plant economy [26].

- **Product Concentrations**

The concentration of various compounds created during the organic break-down process, such as Volatile Fatty Acid, affects the stability of the anaerobic digestion process (VFA). Acetate, propionate, butyrate, lactate, and other fatty acids are produced during the acidogenesis process. When the digester's buffering capability is depleted, an excessive concentration of these acids might cause the pH inside the reactor to plummet. The buffering capacity of the digesters, as well as how they will react to a specific quantity of VFA concentration, differ from one digester to the next, depending on the microbial population [26].

2.2 Lignocellulosic biomass

Lignocellulosic biomass is the dry matter of plants that is mostly made up of cellulose, hemicellulose, and lignin [27]. Lignocellulosic biomass consists mostly of three polymers: cellulose, hemicellulose, and lignin, with minor amounts of additional components such as acetyl groups, minerals, and phenolic substituents. Figure 2.2 shows the lingocellulose's primary components and structures.

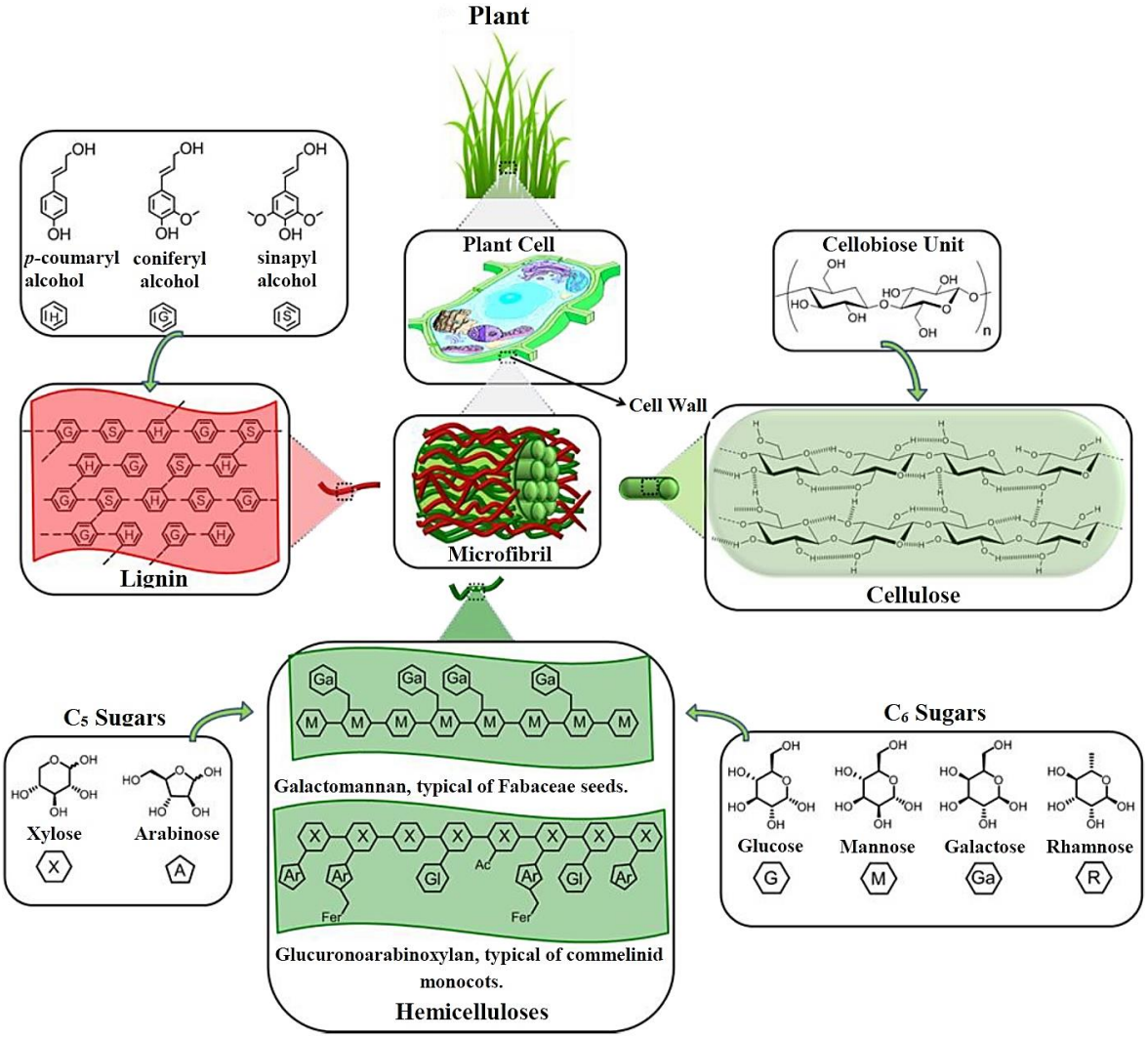

Figure 2.2: The main components and structures of lignocellulose [28].

These polymers are arranged in complex non-uniform three-dimensional structures to varied degrees and relative compositions depending on the type of lignocellulosic biomass.[28]

Lignocellulosic biomass can be transformed into energy or energy carriers using thermochemical or biochemical conversion methods. Thermochemical conversion, which includes combustion, pyrolysis, gasification, and liquefaction, employs heat and chemical processes to produce sources of energy from biomass. Biochemical conversion of biomass entails the breakdown of biomass into gaseous or liquid fuels, such like biogas or bioethanol, using bacteria, microorganisms, or enzymes. Figure 2.3 illustrates common biomass conversion technologies, as well as their principal products and end-uses [27].

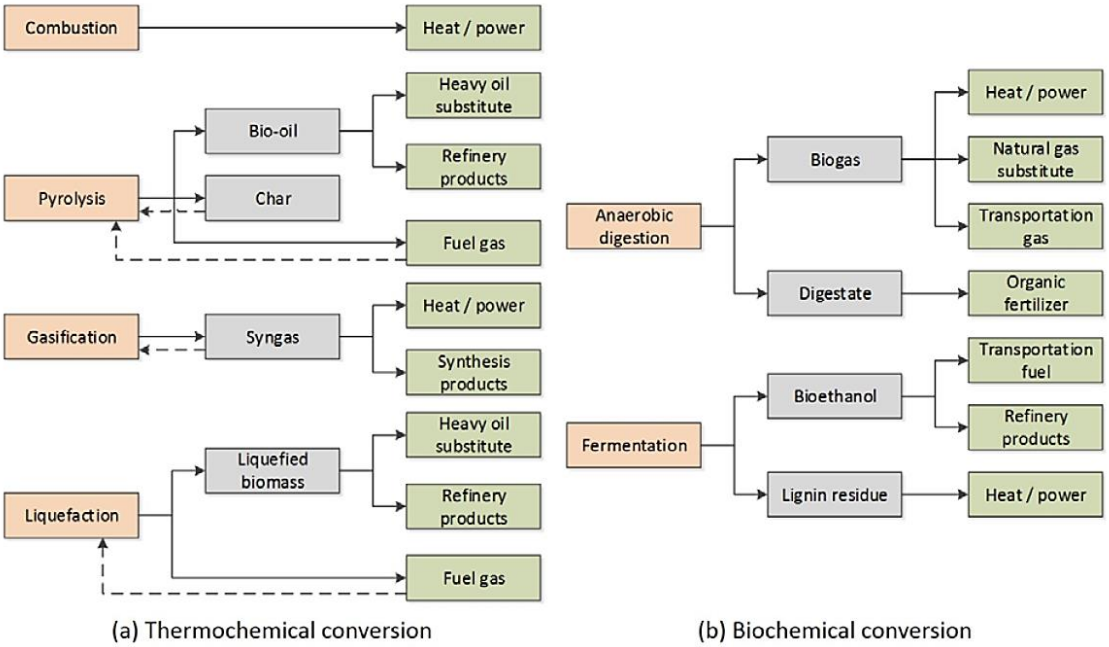

Figure 2.3: Thermochemical and biochemical conversion of lingocellulosic biomass [27].

The crystallinity of cellulose, the hydrophobicity of lignin, and the encapsulation of cellulose by the lignin-hemicellulose matrix have all evolved to make lignocellulose resistant to degradation. Lignocellulosic biomass is primarily made up of cellulose. Because cellulose accounts for over half of all organic carbon in the biosphere, converting it into fuels and useful compounds is favorable. The second most prevalent polymer is hemicellulose. Xylan, galactomannan, glucuronoxylan, arabinoxylan, glucomannan, and xyloglucan are among the heteropolymers that constituted hemicellulose, which has a random and amorphous structure. Thirdly, lignin is a phenylpropanoid-based three-dimensional polymer. It acts as a cellular glue, providing compressive strength to plant tissues and individual fibres, stiffening the cell wall, and insect and pathogen resistance. So, Cellulose is a glucose-based polymer that gives plants structural support, whereas hemicellulose is responsible for binding, and lignin ensures the integrity of the entire stricture [28].

2.2.1 Methods for Treating Lignocellulosic Biomass

Lignocellulose fractionation into its three principal components, cellulose, hemicelluloses, and lignin, is the major aim of lignocellulosic biomass refining [28]. We can transform lignocellulosic biomasses into energy via thermochemical and biochemical processes [14]. Thermochemical and biochemical conversion converts biomass and waste into heat, power, biofuels, chemicals, and biomaterials in a cost-effective and environmentally friendly manner [29]. Due to the presence of lignin, biological fermentation of lignocellulose biomass is challenging. Lignin works as a barrier, preventing the cellulose from being degraded by cellulosic enzymes [30]. The thermochemical method can efficiently and quickly transform biomass into fuels or chemicals. For biomass conversion, many thermochemical processes have been widely utilized, including pyrolysis, gasification, and hydrothermal liquefaction.

Hydrothermal liquefaction and pyrolysis have been identified as two of the most cost-effective and environmentally friendly technologies for biomass conversion among all of these options [31]. Pyrolysis is a thermochemical process of creating biochar, syngas, bio-oil, and aqueous pyrolysis liquid (APL) from dry biomasses [14].

2.3 Thermal hydrolyzed process

The Thermal hydrolyzed process (THP) is a process in the biogas production process that takes place before anaerobic digestion. In the treatment of sewage sludge, thermal hydrolysis refers to processes that take place at high temperatures (from 140 °C to 170 °C) and pressures (from 6 to 9 bar) in the absence of oxidants, before anaerobic digestion. It has been utilized as one of the most effective pre-treatment methods for increasing anaerobic digestion biogas production. High temperature and pressure cause sterilisation of sludge, disintegration of sludge flocs, and rupture of cooked cell membranes. Different temperatures, for example, 145 °C, 175 °C, and 186 °C, 165 °C are reported as effective as THP pre-treatment temperatures. Because these results are contradicting, other aspects should be considered, such as the formation of refractory compounds, the time required to heat the sludge to the desired temperature, and the time required to cool before entering the AD digester. Different THP times have been recorded in terms of reaction time. Despite these findings, several researchers suggest that the optimal reaction time is 30 minutes [32].

2.4 Pyrolysis process

In the absence of oxygen, pyrolysis breaks down chemical bonds to generate new molecules, and it has a lot of flexibility when it comes to processing raw biomass sources into end products [33]. Pyrolysis (Py) converts the lignocellulose matrix into gaseous (syngas), liquid (bio-oil, pyrolysis oil), and solid (biochar) fractions in a single step and without the use of chemical reagents, allowing for the generation of renewable fuels and materials [34]. Solid, gas, and pyrolysis oil are the primary products of the process. Several factors influence yields and composition, including feedstock, particle size, heating rate, temperature, and so on. Slow, fast, and flash pyrolysis are the three types of pyrolysis. Table 2.2 categorizes the processes and some typical yields.

Table 2.2: Typical values for the various pyrolysis processes [35].

Pyrolysis Process	Solid Residence time (s)	Heating Rate (k/s)	Particle Size (mm)	Temperature (k)	Product Yield (%)		
					Pyrolysis Oil	Char	Gas
Slow	450-500	0.1-1	5-50	800-1200	30	35	35
Fast	0.5-10	10-200	<1	1100-1500	50	20	30
Flash	<0.5	>1000	<0.2	1300-1570	75	12	13

Slow pyrolysis is pyrolysis in which the feedstock is heated slowly, usually to a temperature of 800 to 1200k. This is accomplished inside the particle when utilizing large particles in the reactor as the outer layer acts as a heat insulator. This might also be achieved by designing the reactor so that the biomass is heated slowly. Char is the predominant yield in such conditions. Char, also known as biochar, is thought to be mankind's oldest fuel. This was used to heat and extract metals before the discovery of coal. The biomass is heated quickly in fast pyrolysis, mostly to temperatures higher than in slow pyrolysis. Oily liquids are the major yield when the residence time of solids and volatiles is short. The process favors gas over pyrolysis oil as the temperature rises. For producing pyrolysis oil, flash pyrolysis is a viable approach. Oil output from pyrolysis can reach 75%. In short terms, the process can be explained by a quicker heating rate than fast pyrolysis, as well as a shorter feedstock residence time.[35]

In fact, the proportion of bio oil, biochar, and syngas generated vary when process parameters are changed. Char formation is aided by a lower process temperature and a longer vapor residence time. Syngas formation is aided by higher temperatures and longer residence times, but optimal bio oil is produced by moderate temperatures and short vapor residence times [36].

Bio-oil is made up of molecules that are formed when cellulose, hemicellulose, and lignin are broken down. Higher cellulose content produces more liquid products, higher hemicellulose content produces more gas, and higher lignin content produces more solid residues. The bio-oil is separated into aqueous phase (APL) and organic phase due to the high concentration of water in the feedstocks. Depending on the type of biomass, the organic phase (or biocrude) is a complex mixture of oxygenated hydrocarbons and nitrogenated compounds such like sugars, aromatics, ketones, short chain carboxylic acids, phenolics, and furan derivatives. Because of its complicated composition and high oxygen levels, it is difficult to use this organic phase directly in AD, but it has the potential to become a renewable alternative to heavy fuel oil. APL, on the other hand, has a high chemical oxygen demand (COD) concentration as well as a variety of potentially poisonous organic compounds, making it potentially hazardous to the environment if not adequately controlled [37]. Figure 2.4 is a simplified flow diagram illustrating the pyrolysis process concept [38].

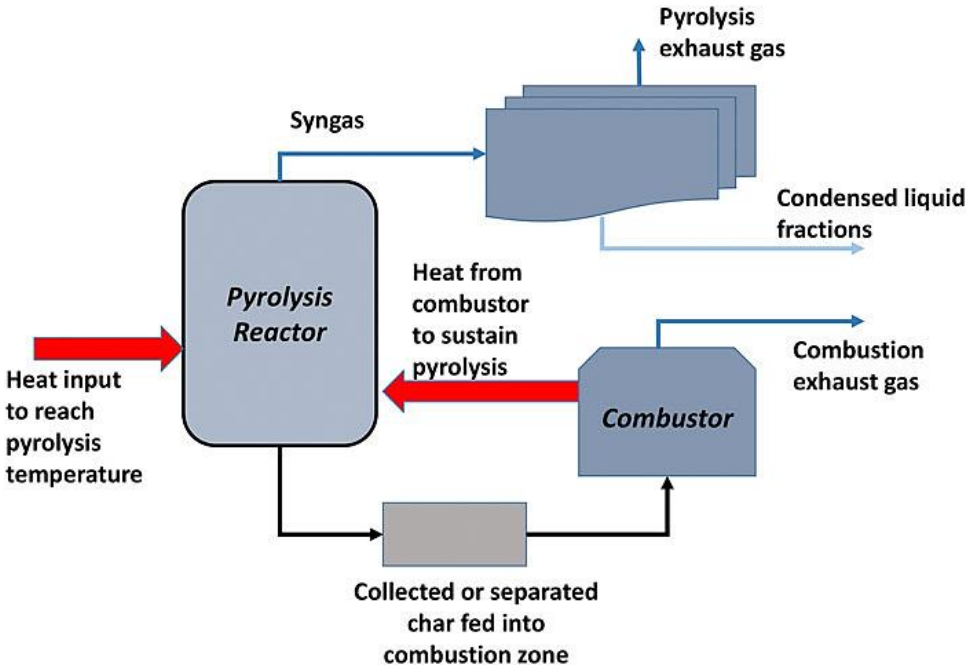

Figure 2.4: The pyrolysis process flow chart in general [38].

2.5 Aqueous Pyrolysis Liquid (APL)

Aqueous pyrolysis liquid (APL) is a high-COD byproduct of wastewater biosolids pyrolysis that contains a wide range of complex organic compounds as well as ammonia nitrogen (NH3-N). APL could be used as a co-digestate in anaerobic digesters to increase biogas production. Some APL organics and NH3-N, on the other hand, are known to hinder methane-producing microorganisms [13]. It cannot be ignited or used directly as fuel due to its low thermal value. Carboxylic acids, aldehydes, phenols, alcohols, ketones, and nitrogenous organics like pyridine, pyridinol, pyrrole, pyrazine, and aminophenol are among the complex organics found in APL. Many APL components are poisonous to mammalian cells and microbes, such as nitrogenous organics. APL yields can be high during some pyrolysis circumstances, accounting for 70–100% of the total weight of the pyrolysis liquids and containing >45 percent of the feedstock biomass carbon [39].

2.6 Syngas

Syngas, also called a synthesis gas, is an energy vector for a sustainable energy future that is produced through thermochemical conversion of various sorts of wastes [40]. Syngas has traditionally been obtained from fossil fuels, although new production techniques, such as syngas from biomass gasification, electrolysis of water, or electrocatalytic CO2 reduction, have lately piqued interest [41].

The content of syngas changes depending on biomass composition and pyrolysis process parameters. H2 and CO are the most common gaseous products formed during pyrolysis. It also contains a little amount of CO2, N2, H2O, a mixture of alkanes, alkenes, and alkynes such CH4, C2H4, C2H6, tar, and ash. The endothermic reaction occurs when the pyrolysis temperature is higher. The vaporization of moisture from the biomass occurs first as pyrolysis

increases. Thermal decomposition and devolatilization follow. Tar is created at this point, and volatile species are released. To form a mixture of syngas, a number of secondary processes such as decarboxylation, decarbonylation, dehydrogenation, deoxygenation, and cracking take place. As a result, higher temperatures facilitate tar decomposition, resulting in the formation of syngas with lower oil and char yields, but with wet biomass, the largest quantity is produced later in the process. This is obvious and expected, as increased humidity leads to longer drying times. At higher temperatures, hydrocarbon cracking creates hydrogen. CO and CO2 are formed as a result of the presence of oxygen in biomass. The evolution of carbonated oxides produced is determined by the presence of an oxygenated polymer called cellulose. In the vapour phase, lighter hydrocarbons such as CH4, C2H4, C2H6, and others are generated by the reforming and cracking of heavier hydrocarbons and tar. Syngas has the advantage of producing a small amount of unburned hydrocarbon (HC) and carbon monoxide (CO) while producing larger nitrogen oxide emissions (NOx). According to reports, CO and H2 in syngas have a higher flame speed and temperature, resulting in higher temperatures in engines and a faster rate of CO2 and NOx production. About 10–35 percent of biogas is produced by slow pyrolysis techniques. Flash pyrolysis produces more syngas at a greater temperature [42].

2.7 Combination of pyrolysis products in anaerobic digestion

Anaerobic digestion and pyrolysis are two potential processes for degrading lignocellulosic biomass and generating a variety of value-added and renewable bioenergy products. The combination of anaerobic digestion and pyrolysis will open up new avenues for integrating biological and thermochemical processes to get more bioenergy from lignocellulosic biomass [43]. Pyrolysis is a thermochemical process that transforms organic waste (including solid digestate from AD) into three primary products: syngas (mostly CO2, H2, and CO), bio-oil (composed of organic and aqueous phases), and biochar. Ordinarily, lignocellulosic biomass is bio converting into biogas (CH4 and CO2) through anaerobic digestion, and in the absence of oxygen, biomass is degrading into syngas (mostly H2 and CO2), bio-oil, and biochar after pyrolysis [44].

Pyrolysis syngas contains hydrogen as one of its key components, which could be transformed to methane biologically rather than through a catalytic chemical process [45], and despite its low calorific value, syngas is nevertheless a desirable source of energy that can be turned into heat or heat/electricity on its own or in combination with biogas in boilers and engines. In the meantime, the organic phase of bio-oil can be combusted in a boiler, diesel engine, or combustion turbine to generate electricity or heat, or upgraded to petroleum products or steam reformed to produce hydrogen fuel [46]. The Py route, which is used downstream of AD, is being intensively researched in order to maximize the value of the solid digestate, which is currently exclusively used for soil applications. Py-to-AD coupling is a new area of research aiming at broadening the feedstock to biologically resistant substrates (wood, paper, sludge) [34]. Due to APL's high chemical oxygen demand (COD) concentration and the presence of potentially dangerous organic chemicals such as cresol, ethylbenzene, phenol, and xylene, APL can be damaging to the environment if not adequately controlled. Because APL has a high concentration of organics (30–300 gCOD/L), including acetic acid (about 25 g/L), one feasible APL management technique is anaerobic digestion, which might be converted to biogas including methane for renewable energy generation [47]. The combination of anaerobic digestion and pyrolysis techniques has the potential to be an innovative energy-biochar

production method that maximizes the sludge energy recovery [48]. When compared to the stand-alone AD process, AD-pyrolysis can increase the electricity benefit by 42 percent [49].

Integration and coupling of biological anaerobic digestion with a thermochemical process like pyrolysis provides an alternative approach that not only allows for higher overall energy efficiency but also allows for the use of different pyrolysis products in the digester to boost bio methane production. Biochar produced by pyrolysis and added to the digester can boost biogas production by 5 to 31 percent [50]. Addition of biochar in the digester can help to minimize ammonia inhibition, support microorganism growth and activity, decrease the lag phase, and so increase biogas generation [51]. The simulation findings reveal that combining the pyrolysis and anaerobic digestion processes yields a 59 percent total efficiency, compared to 52 percent for the anaerobic digestion process alone [46].

2.8 Anaerobic Digestion Model No.1 (ADM1)

The International Water Association (IWA) task group has produced Anaerobic Digestion Model No. 1 (ADM1), which aims to bring together scientific knowledge on anaerobic bioprocesses and unify modeling research. As a result, ADM1 has developed a basic platform for anaerobic digestion modeling and is today the most generally accepted and utilized model. ADM1 includes several steps which include biochemical steps such as disintegration, hydrolysis, acidogenesis, acetogenesis, and methanogenesis, as well as physicochemical steps such as ion association/dissociation and gas–liquid transfer. ADM1 is used to simulate anaerobic digestion of various wasters and wastewaters, including industrial wastewaters, domestic wastewaters, agricultural wastes, and municipal wastewater sludge [52].

Monod kinetics are used to model substrate degradation and biomass growth. First order kinetics represent the disintegration of particle matter and biomass degradation. Biogas generation is also simulated by the model. Ammonium equilibrium, carbonic equilibria, dissociation equilibria for the considered organic acids, and stripping of dissolved gases are all included in the ADM1. The electroneutrality balance is used to compute the pH. It does not, however, consider activity adjustments or ionpairing. In addition, the default version does not account for the precipitation of mineral phases in the digester (such as calcite or struvite). The ADM1 has been utilized in industrial wastewater treatment plant design, diagnosis, and optimization [34]. Anaerobic system is complex and has two main reactions types of Biochemical reactions and Physico-chemical reactions. Intracellular or extracellular enzymes generally catalyze biochemical reactions that act on a pool of physiologically accessible organic material. Extracellular processes include the disintegration of composites (such as dead biomass) into particle constituents and the subsequent enzymatic hydrolysis of these constituents to their soluble monomers. The degradation of soluble materials is mediated intracellularly by organisms, resulting in biomass development and decay. Ion association/dissociation, and gas-liquid transfer are examples of physico-chemical reactions that are not biologically mediated. Precipitation is an additional reaction not covered in the ADM1 [53].

2.8.1 Biochemical Reaction Structure in the ADM1

The model comprises three overall biological (cellular) processes (acidogenesis or fermentation, acetogenesis, or anaerobic oxidation of both VFAs and LCFAs, and

methanogenesis), as well as extracellular (partly non-biological) disintegration and extracellular hydrolysis steps. Figure 2.5 illustrates the biochemical processes included in the anaerobic model [53].

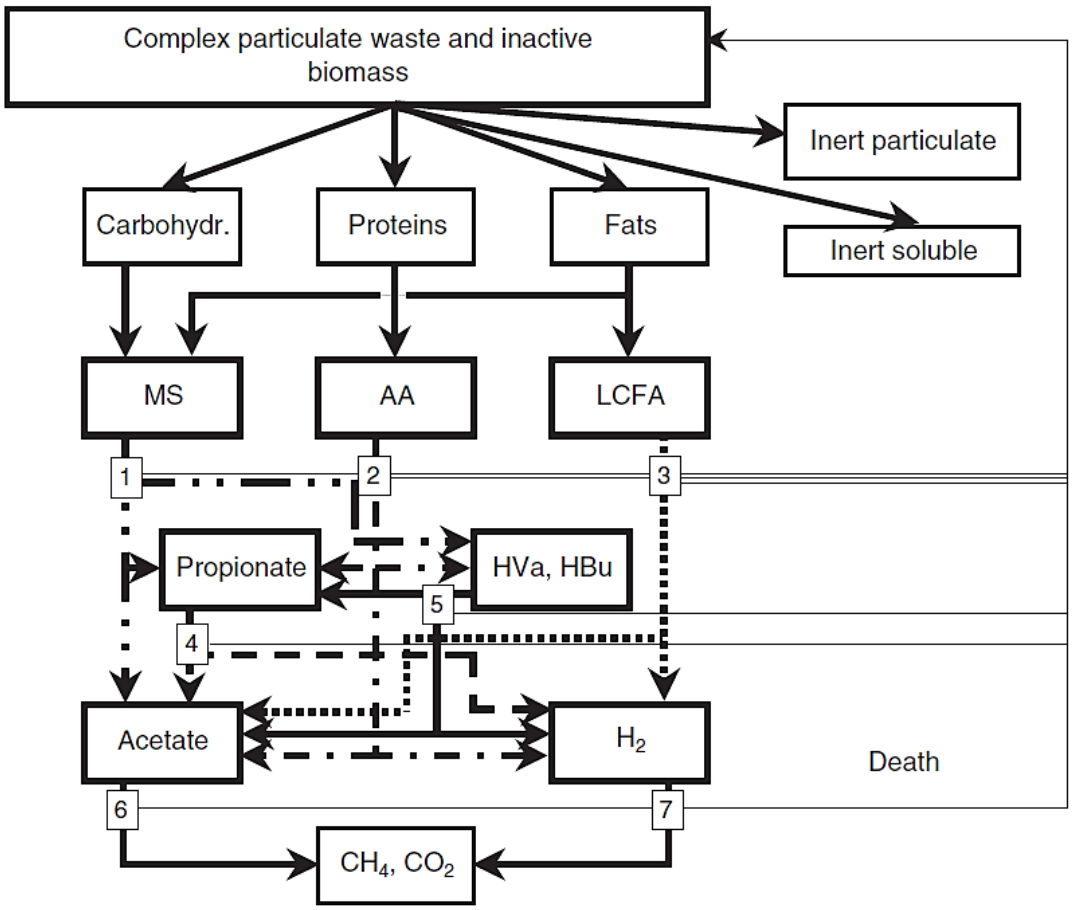

Figure 2.5: Biochemical processes included in the anaerobic model: (1) acidogenesis from sugars, (2) acidogenesis from amino acids, (3) acetogenesis from LCFA, (4) acetogenesis from propionate, (5) acetogenesis from butyrate and valerate, (6) aceticlastic methanogenesis, and (7) hydrogenotrophic methanogenesis [53].

There are several parallel reactions in three of the processes (hydrolysis, acidogenesis, and acetogenesis). The disintegration of complex composite particulate waste into arbohydrate, protein, and lipid particle substrate is considered to be homogeneous. All extracellular biochemical stages were considered to be first order, which is an empiricism-based simplification that reflects the cumulative effect of a multi-step process. The biological kinetic rate expressions and coefficients are described by three expressions uptake, growth, decay in the Appendix E [53].

3 Material and Methods

Lindum's full-scale continuous AD is simulated in different scenarios with and without pyrolysis products as co-substrates. Aquasim application was used for full-scale simulation of Lindum's reactors by using the IWA Anaerobic Digestion Model no.1 (ADM1).
For the first stage the load and concentrations of the substrate from Lindum at year 2014 is used to gain a general simulation and modelling in ADM1. To have more concentration of CH4 and pH, some adjustments were made to alkalinity and ammonium concentrations.
For the next stage, newer loads and concentrations at the year 2021 is used and the volume of reactors assumed 80% of the volume in the starting time, since after some years the walls are thickened by sludge and the effective volume is reduced.

After that adding pyrolysis products in anaerobic digestion is investigated by firstly adding APL as co-substrate, secondly by adding syngas as co-substrate, and thirdly by adding combination of the APL and syngas as co-substrate to the AD reactor feed. Figure 3.1 shows the overall flow diagram of a continuous AD reactor fed syngas from pyrolysis and Aqueous Pyrolysis Liquid (APL) as co-substrates in a full-scale reactor at Lindum.

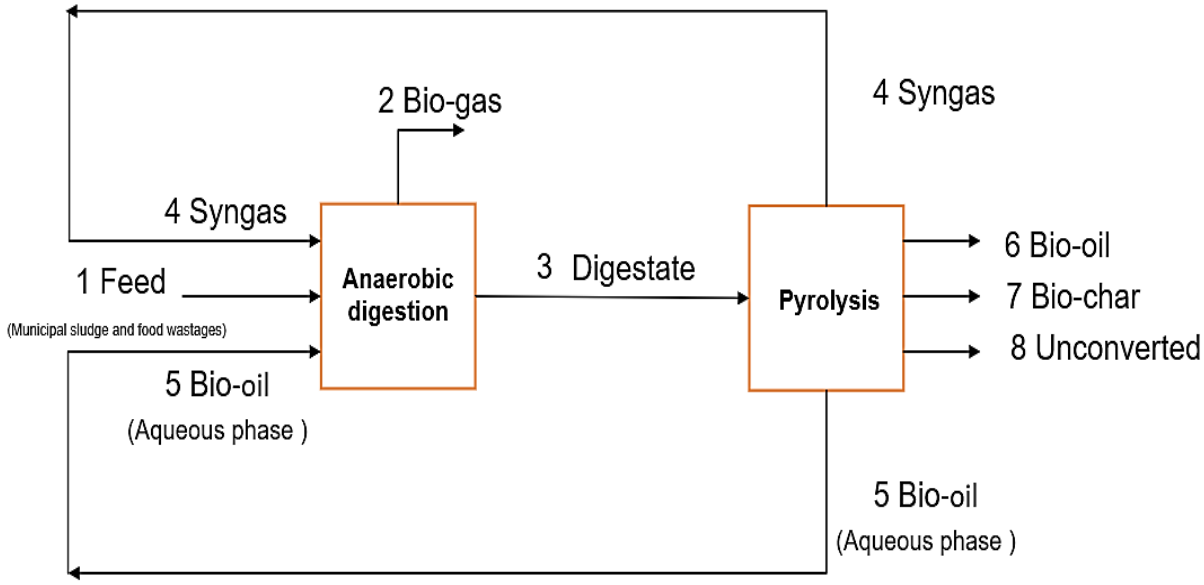

Figure 3.1: Flow diagram of AD reactor with pyrolysis products as co-substrates in anaerobic digestion.

The performance of the pyrolysis process is influenced by a number of factors, including pyrolysis operation conditions, feedstock content, and the types of reactors used.
Other parameters that affect the process include the catalytic loading rate, particle size, carrier gas, and gas flow rate. Quality and product yield can be improved by carefully adjusting the aforementioned parameters during the process [54].
Based on F. Monlau [55] the Digestate pyrolysis (600 ºC) results to 10.2 wt.%, 55.8 wt.%, and 34 wt.% of gas, oil and char. By assuming the total biomass conversion efficiency around 90%, which means 10% of the biomass remains unconverted, and according to Table 3.1 there would be 9.08 wt.%, 50.12 wt.%, and 30.8 wt.% of gas, oil and char respectively.

As 52 % of Bio Oil is in aqueous phase [56], the amount of APL is equal to 52 % of 90.2 which is equal to 52.12 for flow number 5.

Table 3.1: Concentrations, mass flows, and yields of processes.

No. of flow	Flow name	Concentration	Mass flow	Yield [%]
1	Feed to AD	-	202.7 [Lindum]	-
2	Bio gas	-	3 [Lindum]	-
3	Digestate to pyrolysis	100%	200 [Lindum]	-
4	Syngas	9.1%	18.16	9.1
5	Bio oil (Aqueous phase)	52 % of Total Bio Oil [56]	52.12	26
6	Bio oil	48% of Total Bio Oil	48.12	24.1
7	Bio char	30.8%	61.6	30.8
8	unconverted	10%	20	10

The density of syngas is 0.95 kg/m3 [57].
The amount of syngas produced is 18.16 ton per day. Which by considering the density of syngas it would be 19116 m3 syngas produced per day.
Syngas is another product of pyrolysis process which here would be investigated by adding as co-substrate to the to the AD reactor feed. The most important characteristic about syngas is the amount of hydrogen and carbon monoxide it contains, the higher it contains of these two gases, the higher quality the syngas is higher [58]. Table 3.2 shows the Syngas composition during pyrolysis process.

Table 3.2: Syngas composition during pyrolysis process

Syngas composition	Values (%v/v) [55]	g COD material / m3 syngas	kg COD material / m3 syngas
H2	41.40	282.27	0.28
CO	40.50	277.53	0.28
CO2	3.40	0.00145982 mol/l	-
CH4	12.30	337.99	0.34
Other	2.40	-	-

3.1 Basic condition: Modelling and simulation of full-scale operation of Lindum's reactors with full capacity

The first step is a full-scale simulation of Lindum's reactors in 2014. Each reactor has a volume of 1750 m^3, making a total volume of 3500 m^3 for both reactors.

According to the mass balance figure of Lindum in 2014 in Appendix 2, the COD, total solids (TS), and volatile solids (VS) of the wastewater before THP (number 3) and also TS and VS values after THP (number 4) are available. Table 3.3 illustrates the input variables to Lindum's reactors.

Table 3.3: Input variables to Lindum's reactors

Variables	Before THP (3)	After THP (4)
COD (g/L)	174	X
TS (%)	12.9	9.0
VS/TS (%)	62.0	60.0

Having this information, the total COD of hydrolysed sludge can be calculated by using equation (3.1) [59]:

$$\frac{COD_3}{VS_3} = \frac{COD_4}{VS_4} \quad (3.1)$$

$VS_3 = 12.9\% * 62\% = 8\%$ and $VS_4 = 9\% * 60\% = 5.4\%$.

By using equation (3.2) the amount of COD_4 would be 117 g/L which is considered as total COD.

$$COD_4 = \left(\frac{174}{8}\right) * 5.4 = 117.5\ g/L \quad (3.2)$$

- **Soluble COD**

Soluble COD is required in addition to total COD. It is calculated based on lab data and existing THP studies [60] since it is not provided by Lindum.

The ratio of SCOD/TCOD are 0.226 and 0.1781 in Lindum samples and literatures, respectively and their average is 0.202. In the result, the SCOD at Lindum on 2014 is $117.5 * 0.202 = 23.735\ g/L$. Table 3.4 and Table 3.5 illustrate the calculation of TCOD and SCOD, respectively:

Table 3.4: Calculation of TCOD for simulation.

Variables	Before THP	After THP
COD (g/L)	174	117.5
TS %	12.9%	9.0%
VS/TS %	62.0%	60.0%
VS %	8.0%	5.4%
COD/VS (g/L)	2175	

Table 3.5: Calculation of SCOD for simulation.

Variables	Lab Data [Lindum]	Article [60]	THP at Lindum	Digestate at Lindum
TCOD (g/L)	136.02	73	117.5	51
SCOD (g/L)	30.8	13	23.735	10.302
SCOD/TCOD	0.226	0.1781	-	-
Average ratio for SCOD/TCOD	0.202		-	-

- **Volatile Fatty Acids**

Due to the significant experimental error percentage of manual VFA measurement, the amount of volatile fatty acids (VFA) is otherwise estimated. The total VFA of hydrolysed sludge from literature is about 7000 mg acetic acid/L, which should be converted to g COD/L ($kg\ COD/m^3$) to be applied in Aquasimn [60] [53]. Formula of acetic acid is CH_3COOH and equation (3.3) shows its reaction with oxygen: [61]

$$CH_3COOH\ (l) + 2\ O_2(g) \rightarrow 2\ CO_2(g) + 2\ H_2O(l) \quad (3.3)$$

The required oxygen for oxidation of one mole of acetic acid is $2 * 31.999 = 63.998\ g$ [62]. Since the molecular weight of acetic acid is 60.052 g, its chemical oxygen demand is $63.998/60.052 = 1.066\ g$ [61] and so:

$$\frac{7000\ mg\ acetic\ acid/L}{1000} = 7\ g\ acetic\ acid/L$$

$$7\ g\ acetic\ acid/L * 1.066 = 7.462\ g\ COD/L$$

The ratio of VFA/COD is $\frac{7.462}{73} = 0.102$ and since the COD of hydrolysed sludge is 117.5, the total VFA is $117.5 * 0.102 = 12.01\ g\ COD/L$.

Table 3.6 gives an overview of calculation for VFA.

Table 3.6: calculation of VFA in simulation.

Variables	Literature [60]	Lindum
TCOD (g/L)	73	117.5
VFA (mg HAC/L)	7000	-
VFA (g COD/L)	7.462	12.01
VFA/TCOD	0.102	

- **Biodegradability**

The biodegradability of hydrolyzed sludge (HS) has been calculated to be 45% based on available literatures [60] [63]. That means 45% of TCOD (0.45*117.5=52.875 g COD/L) is degraded [61] [62].

- **Inert**

As it is mentioned, 45% of TCOD is degradable. So, the rest of TCOD ((1-0.45) *117.5=64.63 g COD/L) is non-degradable part or inert, which can be soluble or particulate [64].

- **Fatty Acid, Amino Acid, Sugar (Monosaccharides)**

One of the three main stages of anaerobic digestion is hydrolysis, which converts particulate compounds to soluble ones. Carbohydrates, proteins, and lipids are broken down into monosaccharides, amino acids, and fatty acids, respectively, through hydrolysis [19]. In this project, percentage of the new three materials are assumed the same as in basis ADM1.

- **Feed Flow to the Reactor**

Different flow rates of entering waste to the bioreactors are given by Lindum and the average value of one year added to the Aquasim as Input_Qin_dyn.

- **Effluent Data**

In Aquasim the variables with the prefix of 'exp' represents the effluent of the bioreactors, which their values are obtained from Lindum as shown in appendix D.

- **Particulate COD**

Particulate COD is chemical oxygen demand of particulate compounds and estimated as the difference between total COD and soluble COD [65]. Particulate COD can be biodegradable and non-biodegradable. Biodegradable particulate COD is added to the Aquasim as Input_X_C_in and calculated according equation (3.4):

$$Input\_X\_C\_in = (TCOD * biodegradability - total\ VFA - (S\_fa + S\_aa + S\_su))/0.9 \quad (3.4)$$

Table 3.7 gives an overview of input variables in the Modelling and simulation of full-scale operation of Lindum's reactors with full capacity.

Table 3.7: Modelling and simulation of full-scale operation of Lindum's reactors with full capacity

Variables	Unit	Parameters	Value	References
Volume	m^3	-	3500	Lindum
TCOD	kg COD/m^3	-	117.5	Appendix B
Total VFA	kg COD/m^3	input_S_ac_in	13.9	[60] [53]
biodegradability	-	-	0.45	[60] [63]
Total biodegradable	-	-	52.875	[61] [62]

Inert	kg COD/m³	input_X_I_in	64.63	[64]
Applied COD of hydrolyzed sludge	kg COD/m³	input_X_c_in	32.19	
Soluble COD	kg COD/m³	COD_S	23.8	[60]
SCOD - VFA	kg COD/m³	-	10	
Alkalinity	mol/L	input_S_IC_in	0.009292	Appendix C
Ammonium	mol/L	input_S_IN_in (influent)	0.127028	Appendix C
Average feed flow	m³/day	Input_Qin_dyn	203	Lindum
fatty acid	kg COD/m³	Input_S_fa_in	4.37	[73]
amino acid	kg COD/m³	Input_S_aa_in	3.23	[73]
sugar	kg COD/m³	Input_S_su_in	2.1	[73]
real Ch4 flow	m³/day	exp_p_ch4		Appendix D
real gasflow	m³/day	exp_gasflow		Appendix D
real Co2	m³/day	exp_p_co2		Appendix D
TCOD of digestate	kg COD/m³	exp_COD_tot	51	Appendix B
SCOD of digestate	kg COD/m³	exp_COD_S	10.32	Appendix B
carbohydrates	kg COD/m³	Input_X_ch_in	0	
protein	kg COD/m³	Inut_X_pr_in	0	
lipid	kg COD/m³	Input_X_li_in	0	

3.2 Time step zero: Modelling and simulation of full-scale operation of Lindum's reactors with 80% volume of reactors

The modelling and simulation of reactors in Lindum at 2021 with 80% of the volume is the aim of this sub chapter. The volume of reactors is assumed 80% of the volume in the starting time, since after some years the walls are thickened by sludge and the effective volume is reduced.

Here the values of TCOD, SCOD, total VFA, alkalinity, ammonium concentration has been extracted from Lindum experiments. Particulate COD, inert, fatty acid, amino acid, carbohydrates, protein, lipid, and sugar are calculated on the equivalent way to the previous sub chapter.

Table 3.8 gives an overview of input variables in this simulation:

Table 3.8: The added data to Aquasim for 80% volume of reactor.

Variables	Unit	Parameters	Value	References
Volume	m^3		2800	Lindum
TCOD	kg COD/m^3	-	119	Lindum
Total VFA	kg COD/m^3	input_S_ac_in	3.41	Lindum
Biodegradability	-	-	0.45	[60] [63]
Total biodegradable	-	-	53.55	[61] [62]
Inert	kg COD/m^3	input_X_I_in	65.45	[64]
Applied COD of hydrolyzed sludge	kg COD/m^3	Input X_c_in	34.05856	
Soluble COD	kg COD/m^3	COD_S	23.5	Lindum
SCOD - VFA	kg COD/m^3	-	20.09	
Alkalinity	mol/L	Input_S_IC_in	0.0178	Lindum

Ammonium	mol/L	Input_S_IN_in	0.0681	Lindum
Average feed flow	m³/day	Input_Qin_dyn	203	Lindum
Fatty acid	kg COD/m³	Input_S_fa_in	8.77933	[73]
Amino acid	kg COD/m³	Input_S_aa_in	6.48907	[73]
Sugar	kg COD/m³	Input_S_su_in	4.2189	[73]
Real Ch4 flow	m³/day	exp_Ch4		Appendix D
Real gasflow	m³/day	exp_gasflow		Appendix D
Real Co2	m³/day	exp_Co2		Appendix D
TCOD of digestate	kg COD/m³	exp_COD_tot	47	Lindum
SCOD of digestate	kg COD/m³	exp_COD_S	6.04	Lindum
Carbohydrates	kg COD/m³	Input_X_ch_in	0	
Protein	kg COD/m³	Inut_X_pr_in	0	
Lipid	kg COD/m³	Input_X_li_in	0	

3.3 Time step one: Modelling and simulation of Lindum's reactors by adding APL as co-substrate

One of the goals of this project is evaluation the effect of APL pyrolysis products (obtained at 600 ˚C) in bio-gas production by adding them as co-substrate into anaerobic digestion. To better understand the effects of APL during AD, specific simulation examples were used. From table 3.1 the value of APL is given 26 %. In this thesis the essential data of APL at 600 C are extracted from Lindum. However, its biodegradability is found from previous researches, which is 40.8%. (JoëlBlin, 2007) Furthermore, according to researches, the percentage of carbohydrates, protein, lipid and sugar of APL is found and since the utilized APL is wood pyrolysis, the amount of amino acid is assumed 0%. Also, the soluble COD of APL is assumed to be 428 g/L according to the previous research [14]. Table 3.9 shows the input variables of APL in simulation:

Table 3.9: Different variables of APL used for simulation.

Variables	Units	Parameters	Value	References
Volume	m^3		2800	Lindum
TCOD	kg COD/m^3	-	457	Lindum
Total VFA	kg COD/m^3	input_S_ac_in_APL	28.26	Lindum
Applied COD	kg COD/m^3	Input X_c_in_APL	78.81418	Formula
Alkalinity	mol/L	Input_S_IC_in_APL	0	Lindum
Ammonium	mol/L	Input_S_IN_in_APL	0	Lindum
Flow	m^3/day	Input_Qin_dyn_APL	-	Table 3.1
Fatty acid	kg COD/m^3	Input_S_fa_in_APL	52.08612	[73]
Amino acid	kg COD/m^3	Input_S_aa_in_APL	0	[73]
Sugar	kg COD/m^3	Input_S_su_in_APL	35.17712	[73]
Soluble COD	kg COD/m^3		428	[73]
Total hydrolyzed sludge biodegradable	kg COD/m^3	-	53.55	
Biodegradability		-	40.8%	[73]
Total APL biodegradable	kg COD/m^3	-	186.456	[61] [73]
Inert	kg COD/m^3	input_X_I_in_APL	270.544	[73]
SCOD-VFA	kg COD/m^3	-	399.74	
Carbohydrates	kg COD/m^3	Input_X_ch_in_APL	83.90543	[73]
Protein	kg COD/m^3	Inut_X_pr_in_APL	165.9321	[73]
Lipid	kg COD/m^3	Input_X_li_in_APL	62.63926	[73]

3.4 Time step two: Modelling and simulation of Lindum's reactors by adding syngas as co-substrate

In time step two we are aiming to evaluate the effect of Syngas pyrolysis products in bio-gas production by adding them as co-substrate into anaerobic digestion. It has been assumed that the temperature is room temperature (35 ºC), and pressure is 1.1 Pa. In this step the information from table 3.2 were used.

3.5 Time step three: Modelling and simulation of Lindum's reactors by adding combination of syngas and APL as co-substrate

In time step three we are aiming to evaluate the effect of adding combination of syngas and APL as co-substrate into anaerobic digestion, by adding the APL and syngas concentrations from table 3.1, and syngas composition from table 3.2, with the difference that the other gases assumed as CH4 as shown in Table 3.10.

Table 3.10: Syngas composition during pyrolysis process with considering other gases as CH4.

Syngas composition	Values (%v/v) [55]	g COD material / m3 syngas	kg COD material / m3 syngas
H2	41.40	282.27	0.28
CO	40.50	277.53	0.28
CO2	3.40	0.00145982 mol/l	-
CH4	14.70	403.94	0. 40

4 Simulation Results

This chapter presents the results from the simulation of different cases mentioned in chapter 3.

4.1 Simulation result for full-scale operation of Lindum's reactors with full capacity

For simulation of this step the data from Table 3.7 were used. To gain a better adjustment the concentration of alkalinity and ammonium has been changed by trial and error to reach the best adjustment. Figure 4.1 shows the percentage of methane in the gas generated from reactor. The actual methane percentage of full-scale reactor is showed by dots and the simulated methane percentage is represented by solid line.

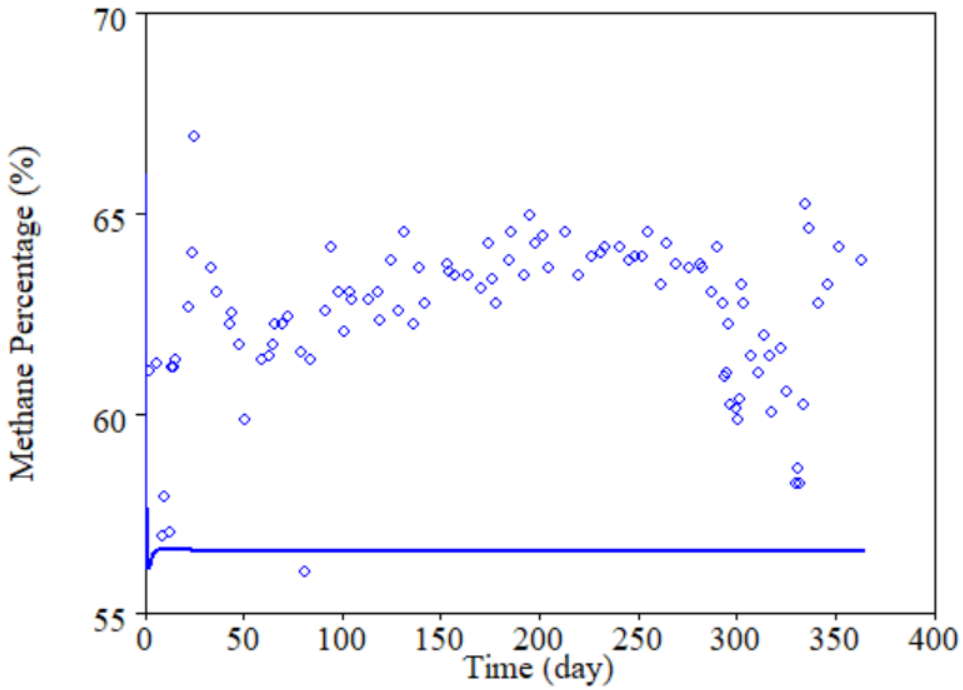

Figure 4.1: Simulated and actual percentage of CH4 values during one year simulation without adjustment.

The actual methane production is higher than the simulated values. So, by some adjustment it has been tried to make the simulated values closer to actual values. By putting more concentration of alkalinity from 0.00929 mol/l to 0.00977 mol/l and ammonium from 0.127028 mol/l to 0.12804 mol/l the concentrations of gas flow and pH would increase. For example, for day 50 the pH values and methane production would reach the value of 7.09, and 56.54% respectively.

Furthermore, to have a better pH, and percentage of methane closer to the actual values of full-scale reactor, the concentration of ammonium has been increased to 0.130 mol/l, the

concentration of alkalinity increased to 0.01 mol/l, and the level of inorganic cation increased from *0.035* to *0.077*. It is noteworthy that the pH and percentage of methane also increased to 7.29, and 58.77 m3/day respectively.

4.2 Simulation of Lindum's reactor with 80% volume capacity at time step zero

For simulation of this step the data from table 3.8 were used. Figure 4.2 shows simulated and actual percentage of methane values during one year simulation. The actual methane percentage of full-scale reactor is showed by dots and the simulated methane percentage is represented by solid line. By having the level of inorganic cation at *0.035*, the percentage of simulated methane percentage is not fit the actual methane percentage.

Also, Figure 4.3 illustrates the simulated pH values, shows in solid line, which is lower than the actual pH values which is showing in dots.

In this case when there is more inorganic cation value with *0.077* the simulated methane percentage and pH values are more than actual values. For example, for day 50 the methane percentage and pH values would increase from 60.48, and 7.26 to 63.08, and 7.43 respectively. In this thesis we put this condition as basic condition.

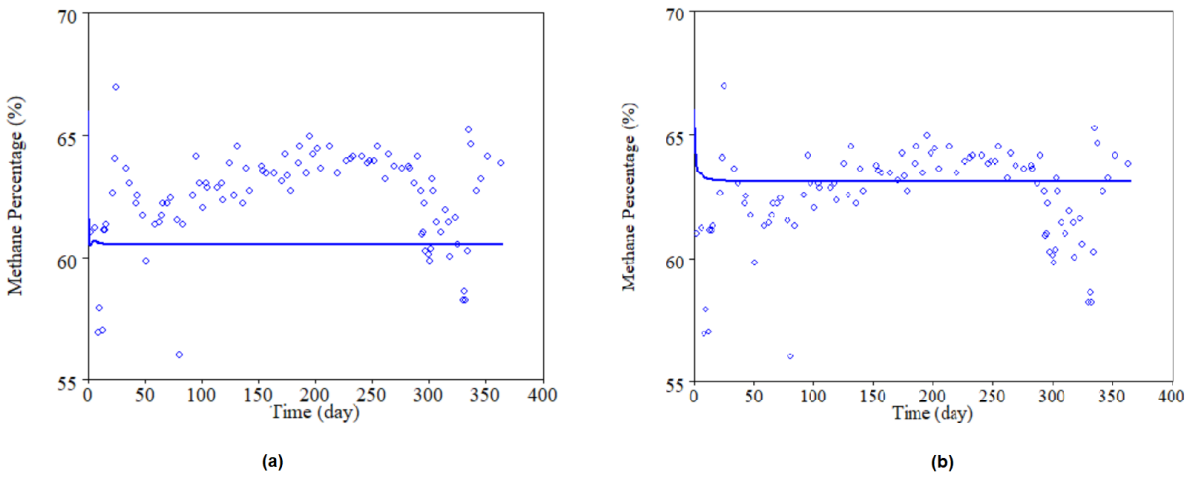

Figure 4.2 Simulated and actual percentage of CH4 values during one year simulation (a), and increased inorganic cation (b).

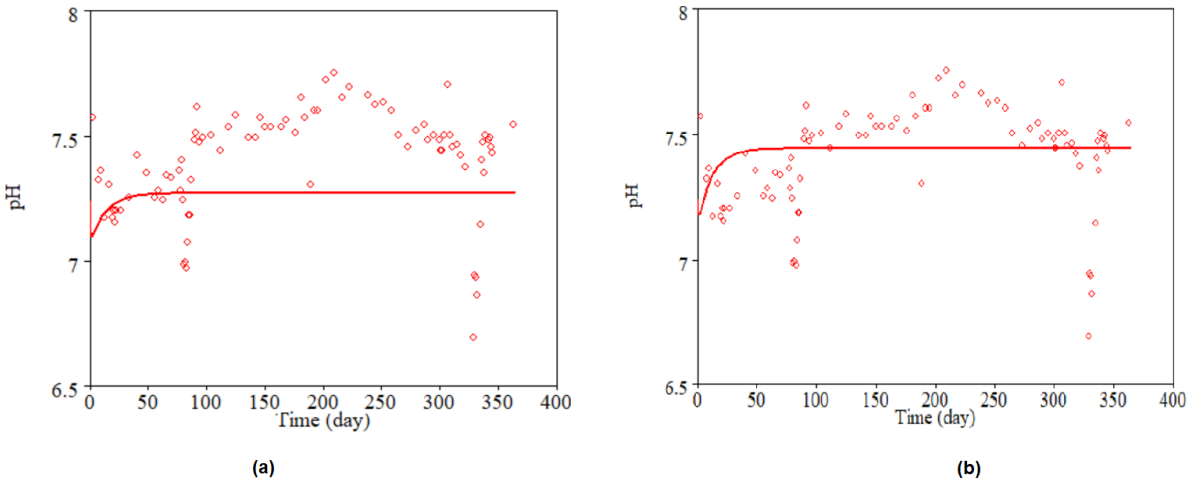

Figure 4.3: Simulated and actual percentage of pH values during one year simulation (a), and with increased inorganic cation (b).

4.3 Simulation of Lindum's reactor at time step one with APL as co-substrate

This subchapter presents the simulation from standard ADM1, by coupling AD with pyrolysis process by adding feed flow of APL to the AD reactor. As shown in table 4.1, by adding 26 % APL, the methane percentage produced in day 50, increases from 63.08 % in time step zero to 63.39 % in time step one, whereas the pH decreases slightly.

Table 4.1 provides the comparison between different values of CH4 and pH for day 50 of simulations in time step zero and one, by coupling AD and pyrolysis process with adding APL produced from pyrolysis process to AD.

Table 4.1: Different values of methane and pH with and without APL at day 50.

Time Step	CH4 (%)	pH
Time step zero	63.08	7.4
Time step one	63.38	7.3

Figure 4.4 and Figure 4.5 illustrate the comparison between different values of CH4 percentage and pH for one-year simulations in time step zero and one.

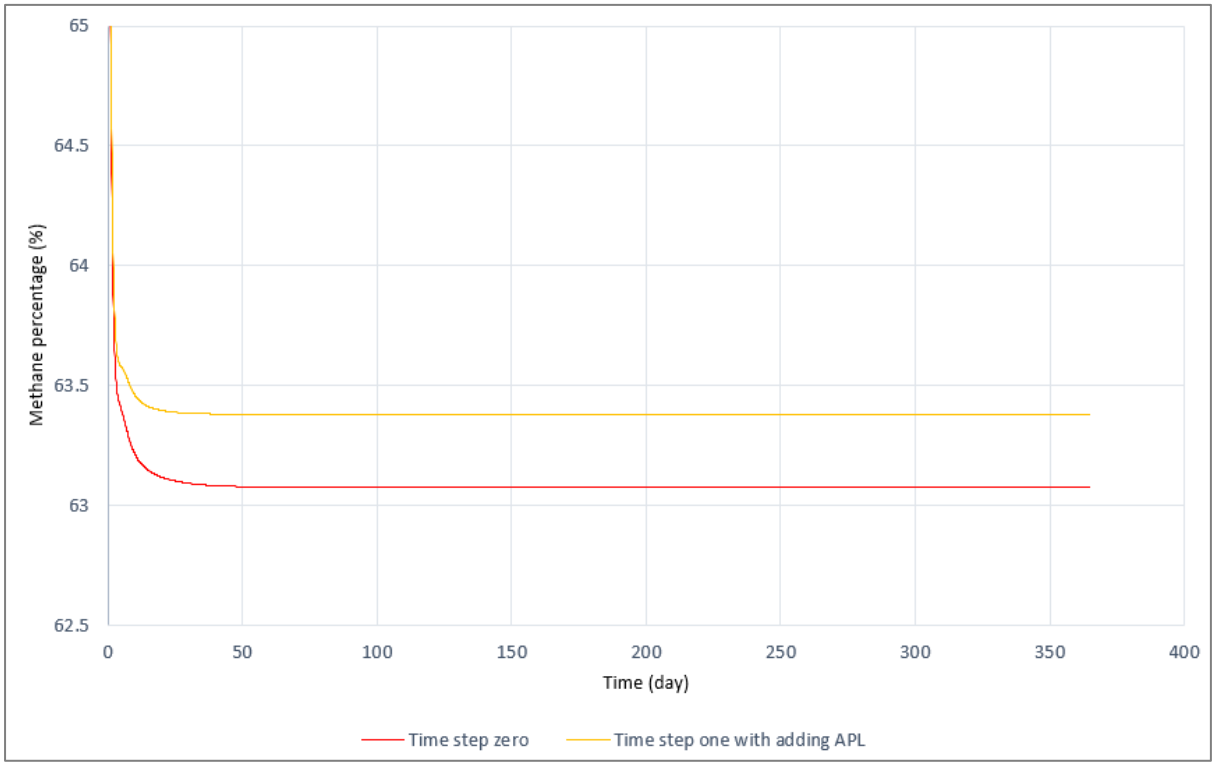

Figure 4.4: Simulated percentage of CH4 of time steps zero and one.

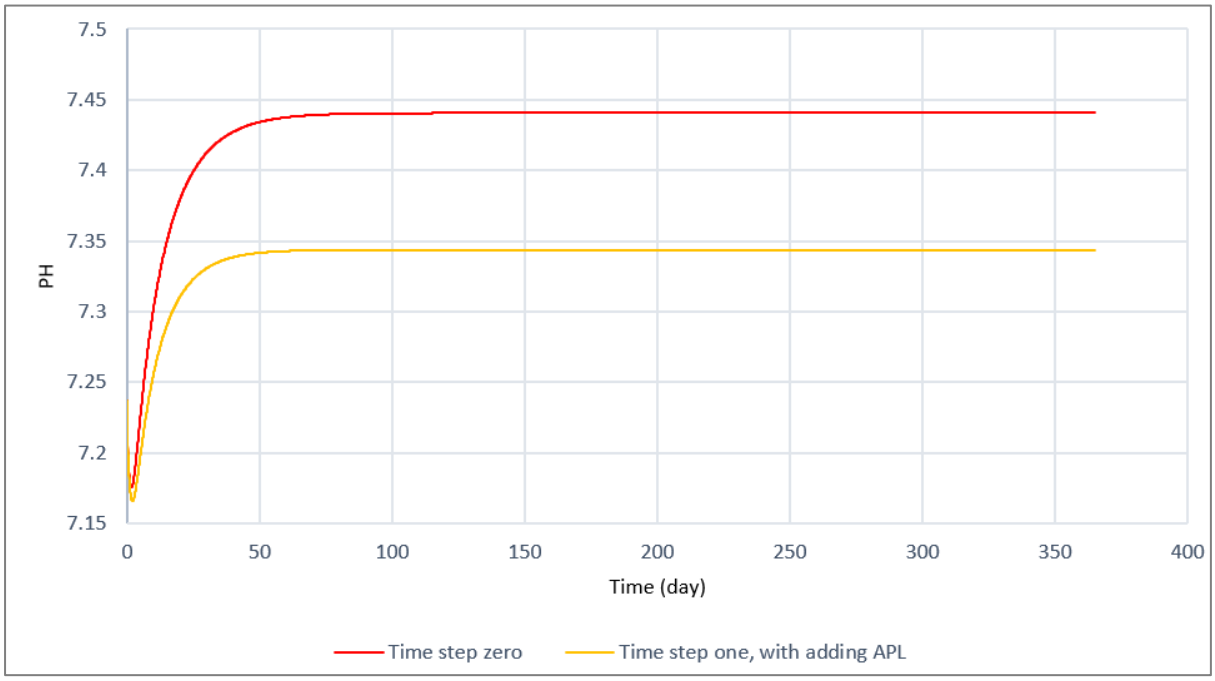

Figure 4.5: Simulated pH values of time steps zero and one.

4.4 Simulation of Lindum's reactor at time step two with syngas as co-substrate

This subchapter presents the simulation from standard ADM1, by coupling AD with pyrolysis process by adding feed flow of Syngas to the AD reactor. The amount of syngas produced is 18.16 ton per day. Which by considering the density of syngas it would be 19116 m3 syngas produced per day. By coupling 100 % amount of produced syngas the methane percentage produced decreases sharply in comparison to time step zero with basic condition of without adding syngas and APL, from about 63 % of methane percentage to about 54 % as shown in Figure 4.6. The pH value is about 7.1.

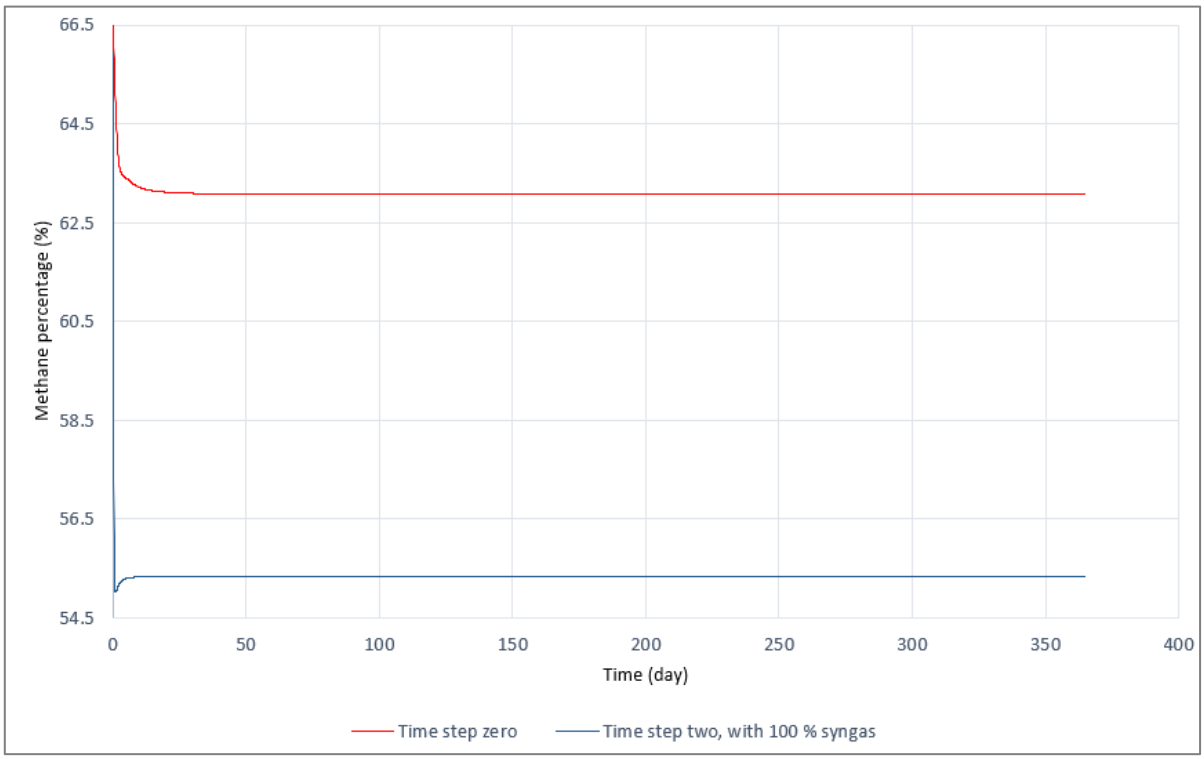

Figure 4.6: Simulated percentage of CH4 of time steps zero and two with 100% syngas.

By reducing the amount of adding average feed flow of syngas to 10 % or 2000 m3/day of average feed flow of syngas based on the compositions of table 3.2, the methane percentage produced is more or less similar to time step zero. Figure 4.7 and Figure 4.8 show the simulations with adding 10 % 0f average feed flow of syngas. As 2.4% of syngas composition are identified as other gases, by considering that as CH4, the amount of CH4 produced is increased slightly more than time step zero. The pH values in these simulations are so close to time step zero as shown in Figure 4.8.

By enhancing hydrogenotrophic methanogenesis, hydrogen has the positive impact of upgrading methane output [67]. There are some studies on producing hydrogen-rich syngas. For example, Kaiqi Shi found that the combining of activated carbon enabled reforming and microwave assisted pyrolysis promotes biomass conversion to H2-rich gas and improves energy conversion efficiency [68]. Also, Yanjie Wang, for example, utilized biochar residues

as catalysts and catalyst carriers to facilitate in-line catalytic reforming following biomass pyrolysis for the production of hydrogen-rich syngas and discovered that biochar offers catalytic activity and a large specific surface area, making it an ideal catalyst carrier for biomass reformation to make syngas [69]. Further works should be done on producing hydrogen-rich syngas. The process of methanogenesis is aided by the presence of hydrogen, which causes hydrogenotrophic microbes to bind H2 to CO2 and convert it to methane to increase methane percentage produced [72].

$$4H_2 + CO_2 \leftrightarrow CH_4 + 2H_2O \tag{4.1}$$

By assuming 86% H_2, 7% CO, and 7% CO2 [70] the amount of methane produced is increasing exponentially by 4 percent more than time step zero. Figure 4.7 and Figure 4.8 illustrate that by adding hydrogen rich-syngas the methane percentage produced is increasing by about 4 percent, and the pH value is increasing to 7.5.

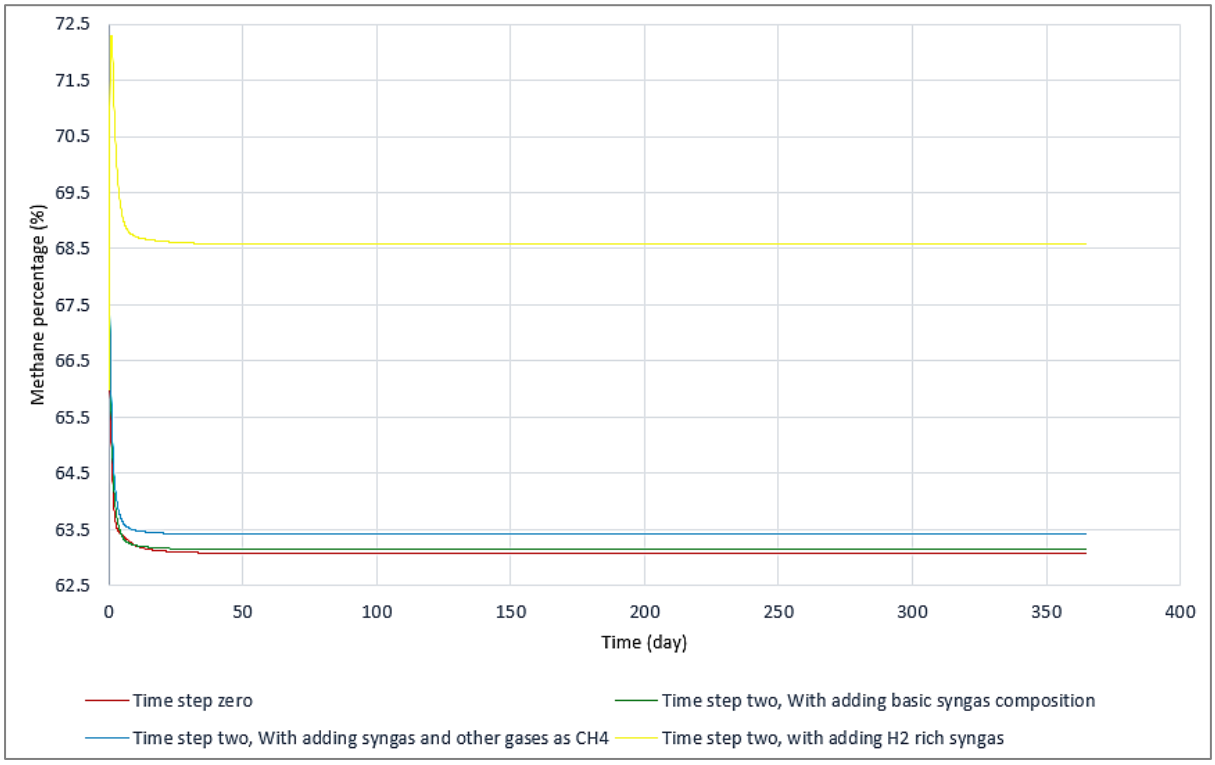

Figure 4.7: Simulated percentage of CH4 of time steps zero and two.

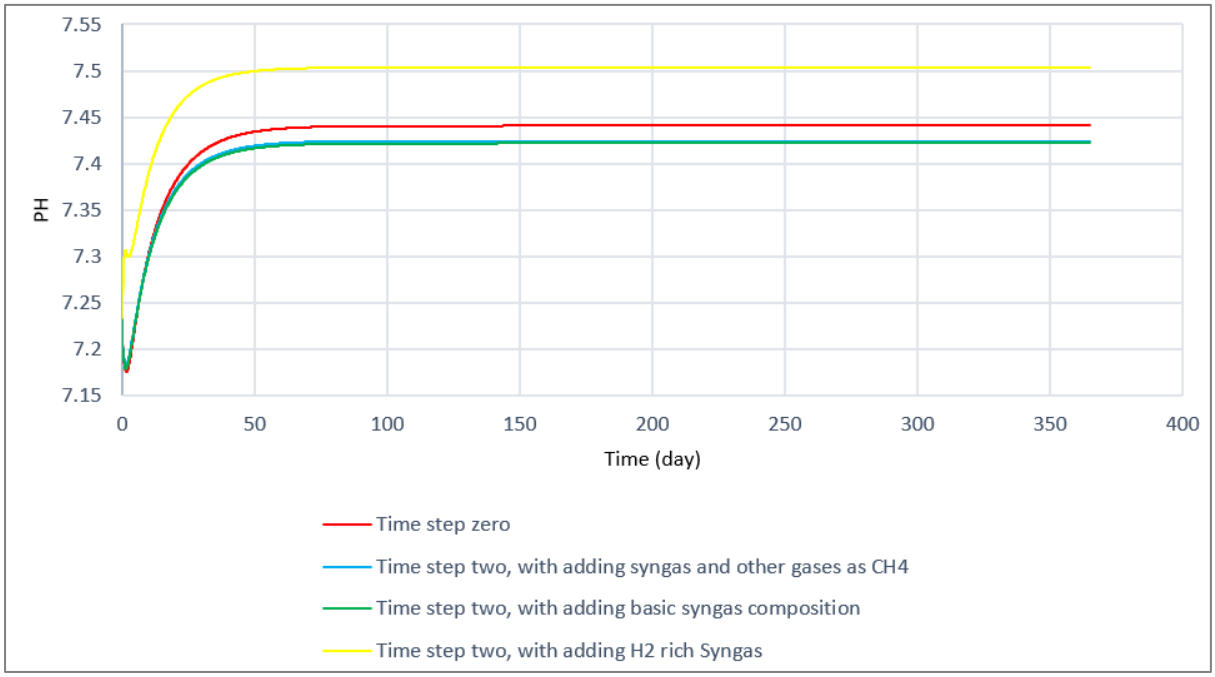

Figure 4.8: Simulated pH values of time steps zero and two.

4.5 Simulation of Lindum's reactor at time step three with combination of syngas and APL as co-substrates

In this step coupling the combination of syngas and APL is simulated in standard ADM1. Here by adding 10% syngas as previous step (time step two), along with APL, the amount of methane percentage is decreased about 10% from about 63% in time step zero to about 55%, as shown in Figure 4.9. The Figure 4.10 shows the simulated pH values of time steps zero and three with 10% syngas during one year simulation which is about 2 % less than in time step zero, and pH value about 0.2% less than time step zero as shown in Figure 4.10.

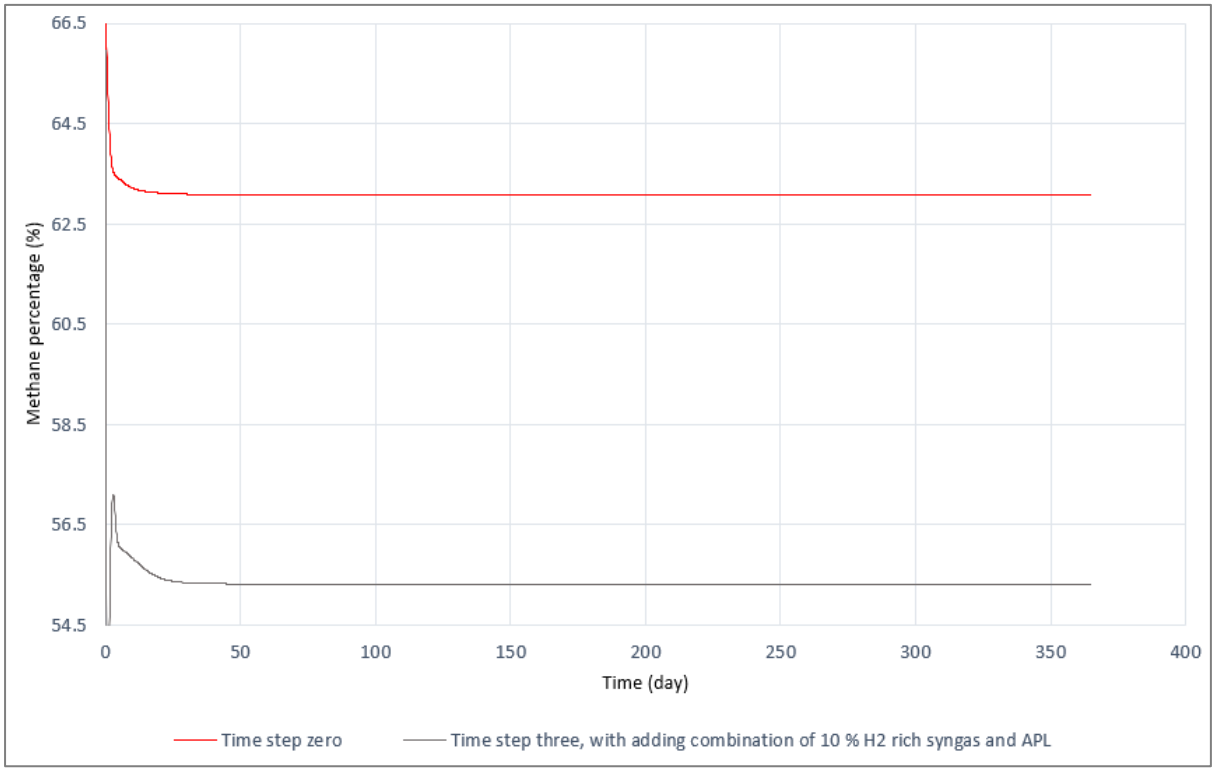

Figure 4.9: Simulated percentage of CH4 of time steps zero and three with 10 % syngas.

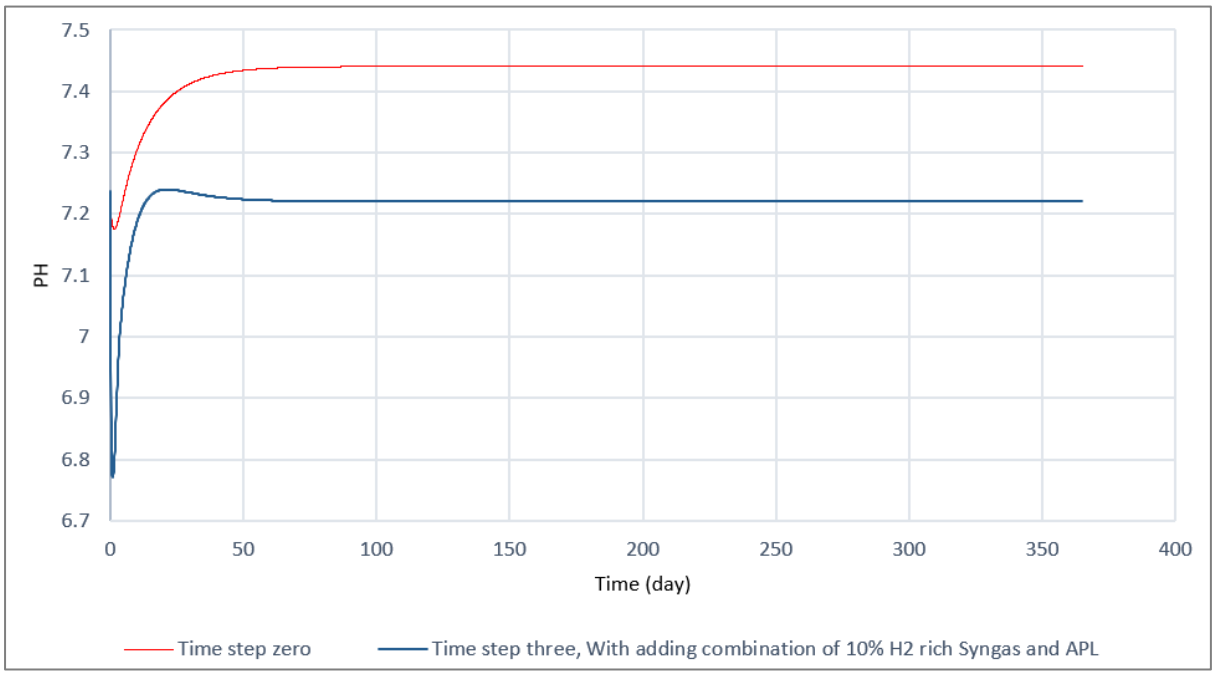

Figure 4.10: Simulated pH values of time steps zero and three with 10% syngas.

By coupling 100% amount of produced syngas along with APL to the AD reactor the methane percentage produced increases from 63% in time step zero to about 65%, as shown in Figure 4.11. Figure 4.12 illustrates that the pH increases from about 7.2 to about 7.4.

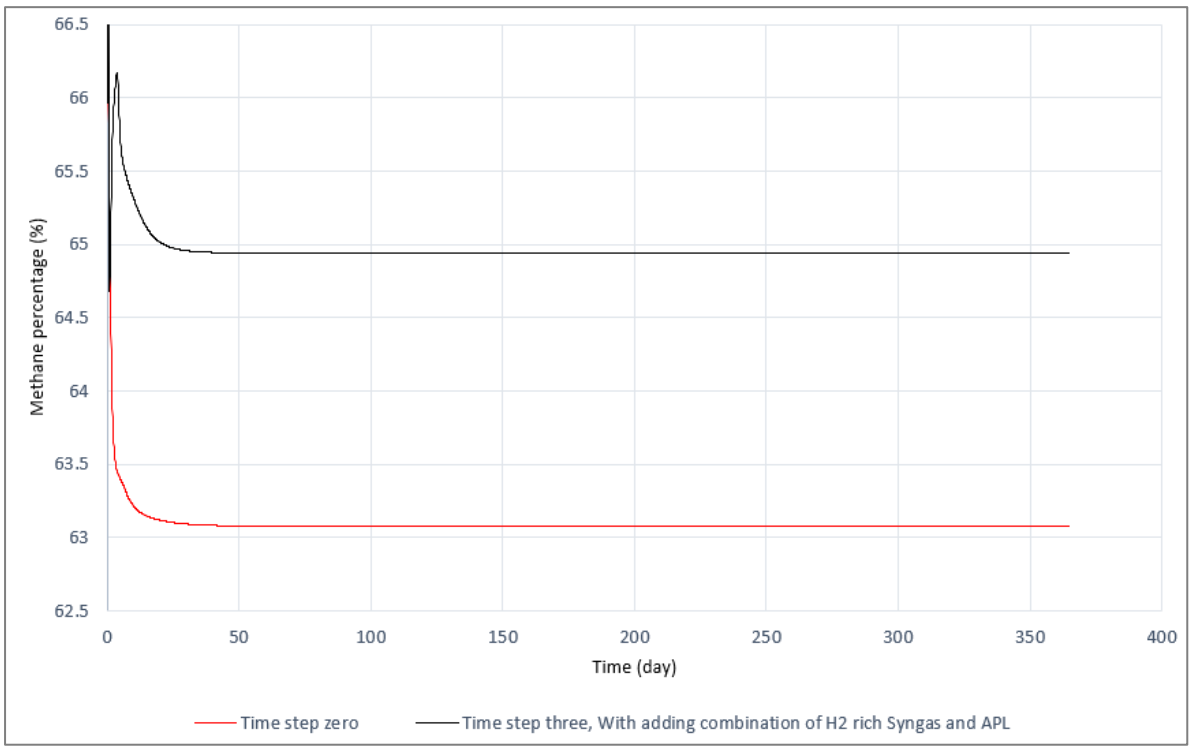

Figure 4.11: Simulated percentage of CH4 of time steps zero and three.

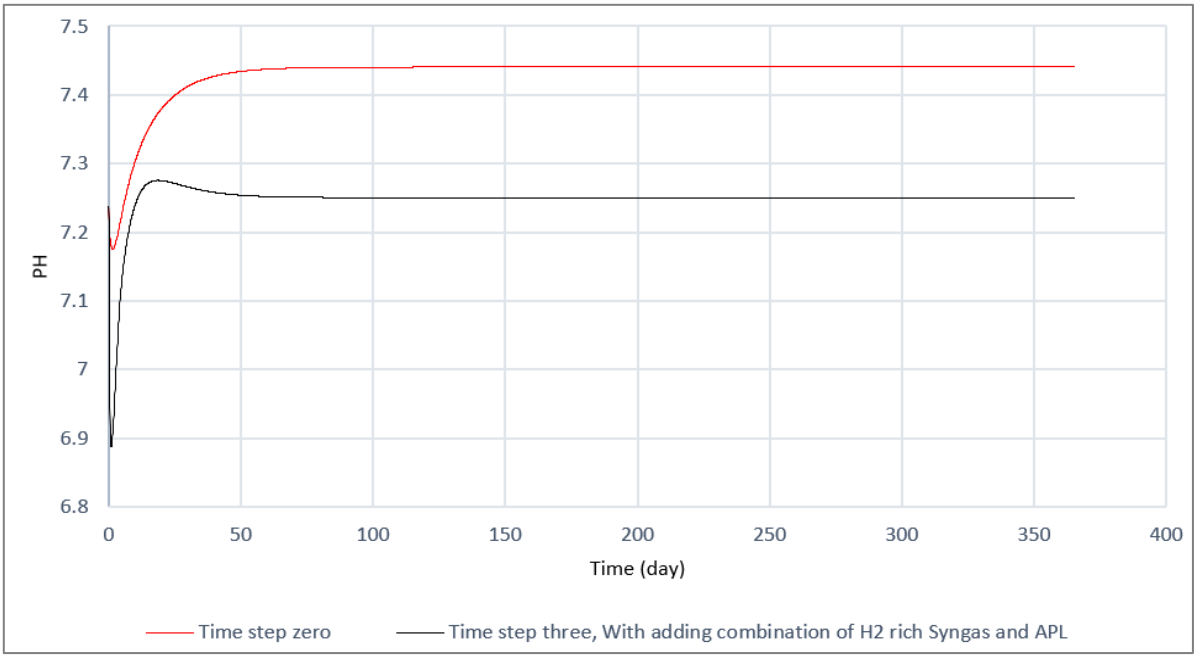

Figure 4.12: Simulated pH values of time steps zero and three.

5 Discussion

In this chapter the simulation of full-scale conditions in different time steps with addition of APL, Syngas, and combination of syngas and APL as co-substrate to the AD reactor are discussed. Figure 5.1 and Figure 5.2 show the overall simulation results of percentage of produced CH4 and pH of different time steps during one year simulation, respectively. Also, Table 5.1 gives an overview of different values of percentage of produced CH4 and pH at day 50 of different time steps and assumptions

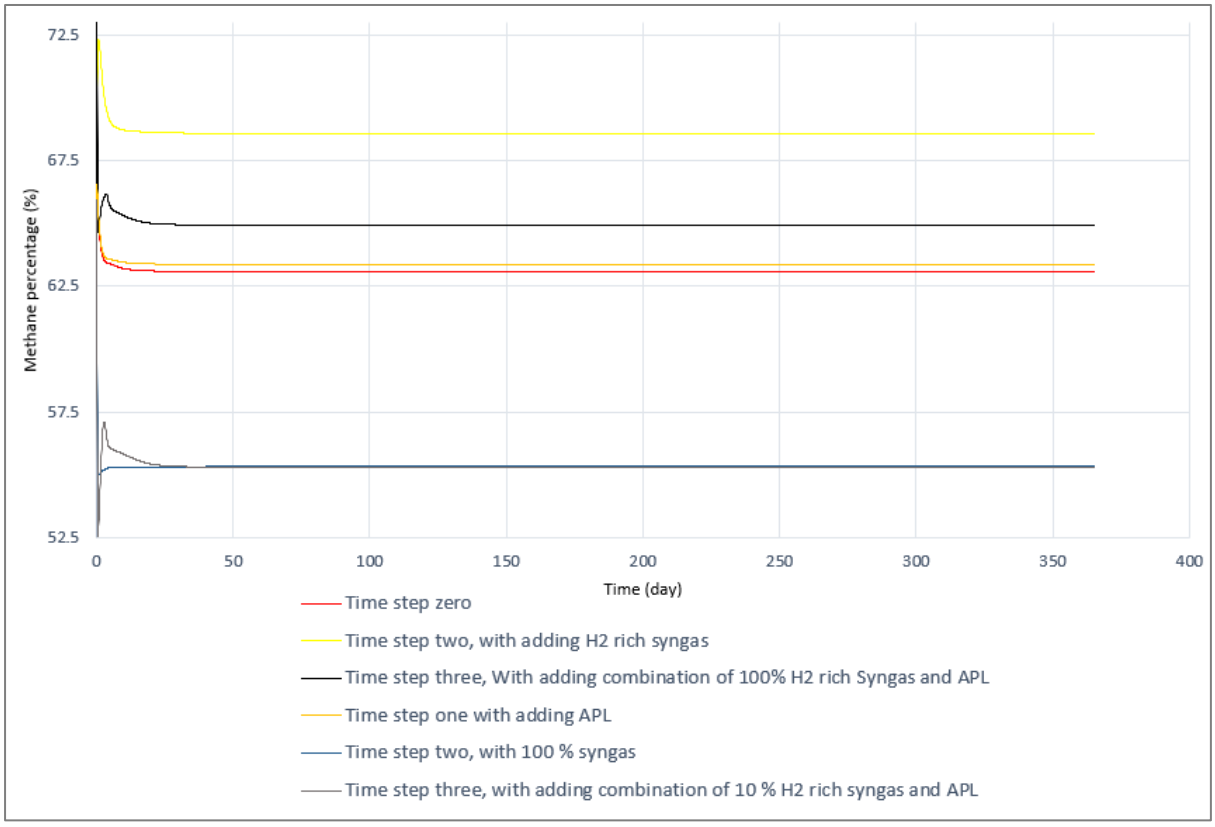

Figure 5.1: Simulated percentage of CH4 of different time steps during one year simulation

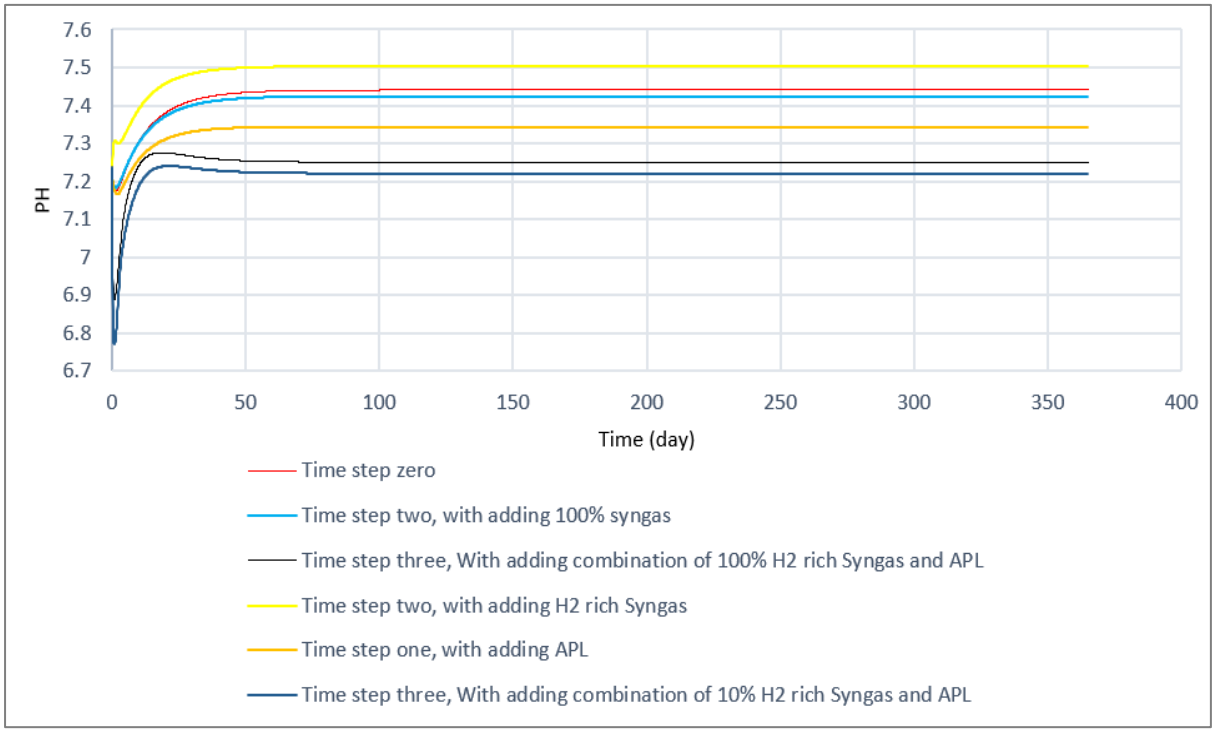

Figure 5.2: Simulated pH values of different time steps during one year simulation.

Table 5.1: Percentage of methane produced and pH value at day 50 in different time steps

Time steps and conditions	Percentage Methane produced	pH
Time step zero	63.07	7.43
Time step one with APL	63.38	7.34
Time step two, with 100 % syngas	55.33	7.41
Time step two, with H2 rich syngas	68.58	7.49
Time step three, with combination of 10% H2 rich syngas and APL	55.31	7.22
Time step three, with combination of 100% H2 rich Syngas and APL	64.94	7.25

5.1 Addition of APL, and Syngas separately as co-substrate to the AD reactor

In time step one the APL added to the AD reactor as co-substrate and investigated its effect in the simulation into ADM1 model. Based on the simulations, addition of APL as co-substrate leads to the about 0.31 percent increases of methane percentage produced. This is whereas the pH value decreases by 0.1.

In time step two the syngas added to the AD reactor as co-substrate. Coupling 100% of produced syngas during pyrolysis process to the AD reactor leads to the reduction in produced methane percentage by 9% in comparison to time step zero. The pH value decreases by 0.3.

By reducing the addition of syngas to 10% into the AD reactor the methane percentage produced becomes more or less similar to time step zero. Hydrogen-rich syngas through process of methanogenesis by binding H2 to CO2 and convert it to methane leads to increase methane percentage produced. By coupling Hydrogen-rich syngas with 86% H_2, 7% CO, and 7% CO2 the methane percentage produced increases by 4% in comparison to time step zero. The pH value increase by about 0.1. Hydrogen offers benefits and drawbacks when it comes to biogas upgrading. In the biogas reactor, hydrogen consumes CO2, resulting in an increase in CH4 production and a reduction in CO2 emissions [71]. However, in this time step with addition of syngas the amounts pf methane produced increases exponentially in comparison to other time steps but because of the increased pH, it may have a negative impact on the anaerobic process. To keep the pH within acceptable ranges, specific solutions are required, such as co-digestion with acidic substrates or pH control [72].

5.2 Addition the combination of syngas and APL as co-substrates to the AD reactor

In time step three the combination of syngas and APL added to the AD reactor as co-substrate. Adding 10% syngas of time step two along with APL causes 10% reduction in methane percentage produced. The pH value decreases by 0.2. By increasing the addition of syngas from ten percent to 100% of produced syngas to the AD reactor the methane percentage produced increases by 2% in comparison to time step zero. The pH value still decreases by 0.2 in an acceptable value of 7.25.
As the table 4.2 gives an overview of all different time steps and conditions, time step two with addition of ten percent hydrogen rich syngas produced the most methane percentage, following by time step three, with combination of 100% H2 rich Syngas and APL. In all mentioned time steps and conditions, the pH value stays in an acceptable range between 7.2 and 7.5.

6 Conclusion

A study has been carried out on the Coupling anaerobic digestion and pyrolysis processes, using Anaerobic Digestion Model No. 1 (ADM1) as base model and modified to simulate, evaluate, and maximize methane production rate in coupling pyrolysis products of APL, and syngas to AD.

Addition of APL as co-substrate to the AD showed a 0.31% increase in methane production in comparison to condition without co-substrate addition. Coupling syngas as another by-product of pyrolysis process was also investigated and simulated. Addition of all syngas produced as co-substrate to AD led to 9% reduction in methane produced. Reducing the amount of addition syngas to the AD was also simulated. Simulations showed that by coupling 10% of syngas as co-substrate to the AD the percentage methane produced becomes more or less similar to the condition of without co-substrate addition. Furthermore, addition of syngas with different compositions as hydrogen-rich syngas was investigated as well. By using hydrogen-rich syngas with 86% H2, 7% CO, and 7% CO2 in AD the methane percentage produced increased by 4%. Finally, simulations related to coupling combination of syngas and APL added to the AD reactor as co-substrate showed 10% reduction in methane percentage produced by adding 10% syngas along with APL. It was while by increasing the addition of syngas from ten percent to 100% of produced syngas to the AD reactor the methane percentage produced increased by 2%. In all mentioned time steps and conditions, the pH value kept in an acceptable range between 7.2 and 7.5.

7 Suggestion for future work

Pyrolysis and anaerobic digestion integration is a novel and rising research topic. There are certain alternatives that might be investigated in order to gain a better grasp of the subject. Following are recommendations for future work:

Since some input variables are based on experiment on Lindum and some others are assumed from previous researches, in order to have more accurate simulations with a lower error rate, more lab experiments should be done and the data specific to reactor operating condition should be measured and used.

- In pyrolysis process, the percentage of unconverted biomass should be studied and measured precisely on Lindum reactors.
- As this study is the coupling pyrolysis products to AD the yields of pyrolysis products such as APL, and syngas should be measured precisely on Lindum reactors.
- Syngas compositions concentration during pyrolysis process should be measured based on Lindum operating conditions at Lindum plant.
- More studies and experiments should be done on producing hydrogen-rich syngas based on Lindum pyrolysis process. Also, the hydrogen rich syngas compositions should be measured precisely.

References

[1] P. Venkateswara Rao, S. S. Baral, . D. Ranjan and M. Srikanth , "Biogas generation potential by anaerobic digestion for sustainable energy," *Renewable and Sustainable Energy Reviews,* vol. 14, no. 7, September 2010.

[2] I. E. Agency, "World Energy Outlook (WEO)," International Energy Agency, France, 2021.

[3] M.-A. Perea-Moreno, E. Samerón-Manzano and A.-J. Perea-Moreno, "Biomass as Renewable Energy: Worldwide Research Trends," *Sustainability,* vol. 11, February 2019.

[4] M. Balat and G. Ayar, "Biomass Energy in the World, Use of Biomass and Potential Trends," *Energy Sources,* 2005.

[5] I. F. Corporation, "Converting Biomass to Energy, A Guide for Developers and Investors," International Finance Corporation, Washington, D.C., 2017.

[6] P. McKendry, "Energy production from biomass (part 2): conversion technologies," *Bioresource Technology,* vol. 83, pp. 47-54, 2002.

[7] H. Al-Haj Ibrahim, Introductory Chapter: Pyrolysis, London: Intechopen, 2020, p. 122.

[8] M. I. Jahirul, M. G. Rasul, A. A. Chowdhury and N. Ashwath, "Biofuels Production through Biomass Pyrolysis—A Technological Review," *energies,* vol. 5, pp. 4952-5001, 2012.

[9] A. O. Ayeni, O. A. Adeeyo, O. M. Oresegun and T. E. Oladimeji, "Compositional analysis of lignocellulosic materials: Evaluation of an economically viable method suitable for woody and non-woody biomass," *American Journal of Engineering Research (AJER),* vol. 4, no. 4, pp. 14-19, April 2015.

[10] P. Kumar, D. M. Barrett, M. J. Delwiche and P. Stroeve, "Methods for Pretreatment of Lignocellulosic Biomass for Efficient Hydrolysis and Biofuel Production," *American Chemical Society,* March 2009.

[11] Z. Echresh Zadeh, A. Abdulkhani, O. Aboelazayem and B. Saha, "Recent Insights into Lignocellulosic Biomass Pyrolysis: A Critical Review on Pretreatment, Characterization, and Products Upgrading," *processes,* July 2020.

[12] D. Kim, "Physico-Chemical Conversion of Lignocellulose: Inhibitor Effects and Detoxification Strategies: A Mini Review," *Molecules,* vol. 23, no. 2, p. 309, February 2018.

[13] S. Seyedi, K. Venkiteshwaran and D. Zitomer, "Toxicity of Various Pyrolysis Liquids From Biosolids on Methane Production Yield," *Front. Energy,* vol. 7, February 2019.

[14] D. Raya, N. Ghimire, G. Ø. Flatabø and W. H. Bergland, "Anaerobic Digestion of Aqueous Pyrolysis Liquid in ADM1," in *The First SIMS EUROSIM Conference on Modelling and Simulation, SIMS EUROSIM 2021, and 62nd International Conference of Scandinavian Simulation Society, SIMS 2021*, Finland, 2022.

[15] L. Chen and H. Neibling, "Anaerobic digestion basics," *University of Idaho extension,* 2014.

[16] P. Huber, C. Neyret and E. Fourest, "Implementation of the anaerobic digestion model (ADM1) in the PHREEQC chemistry engine," *Water Science & Technology,* pp. 1090-1103, MAy 2017.

[17] "Anaerobic digestion process: technological aspects and recent developments," *International journal of Environmental Science and Technology,* May 2018.

[18] A. Anukam, A. Mohammadi, M. Naqvi and K. Granström, "A Review of the Chemistry of Anaerobic Digestion: Methods of Accelerating and Optimizing Process Effciency," *processes,* August 2019.

[19] M. &. E. Inc, Wastewater Engineering: Treatment and Resource Recovery, New York, NY: McGraw-Hill Professional, 2003.

[20] J. N. Meegoda, B. Li, K. Patel and L. B. Wang, "A Review of the Processes, Parameters, and Optimization of Anaerobic Digestion," *International Journal of Environmental Research and Public Health,* October 2018.

[21] M. H. Gerardi, The Microbiology of Anaerobic Digesters, New Jersey, Hoboken: John Wiley & Sons, Inc, 2003.

[22] J. del Real Olvera and A. L. Lopez, Biogas Production from Anaerobic Treatment of Agro-Industrial Wastewater, Biogas, D. S. K. (Ed.), Ed., InTech, 2012.

[23] E. Nie, P. He, H. Zhang, L. Hao, L. Shao and F. Lü, "How does temperature regulate anaerobic digestion?," *Renewable and Sustainable Energy Reviews,* July 2021.

[24] A. Eugen Cioabla, I. Ionel, G.-A. Dumitrel and F. Popescu, "Comparative study on factors affecting anaerobic digestion of agricultural vegetal residues," *Biotechnol Biofuels,* p. 5:39, June 2012.

[25] J. Lin Chen, R. Ortiz, T. Steele and D. Stuckey, "Toxicants inhibiting anaerobic digestion: A review," *Biotechnology Advances,* p. 1523–1534, October 2014.

[26] T. Al Seadi, D. Rutz, H. Prassl, M. Köttner, T. Finsterwalder, S. Volk and R. Janssen, Biogas Handbook, T. A. Seadi, Ed., University of Southern Denmark Esbjerg, 2008.

[27] J. Cai, J. He, X. Yu, S. W. Banks, Y. Yang, X. Zhang, Y. Yu, R. Liu and A. V. Bridgwater, "Review of Physicochemical Properties and Analytical Characterization of Lignocellulosic Biomass," *Renewable and Sustainable Energy Reviews,* vol. 76, pp. 309-322, September 2017.

[28] F. H. Isikgor and C. R. Becer, "Lignocellulosic Biomass: A Sustainable Platform for Production of Bio-Based Chemicals and Polymers," *Polymer Chemistry*, May 2015.

[29] A. Trubetskaya and L. Matsakas, "Special Issue: Biochemical and Thermochemical Conversion Processes of Lignocellulosic Biomass Fractionated Streams," *processes,* May 2021.

[30] D. Fabbri and C. Torri, "Linking pyrolysis and anaerobic digestion (Py-AD) for the conversion of lignocellulosic biomass," *Current Opinion in Biotechnology,* vol. 38, pp. 167-173, April 2016.

[31] W.-J. Liu and H.-Q. Yu, "Thermochemical Conversion of Lignocellulosic Biomass into Mass-Producible Fuels: Emerging Technology Progress and Environmental Sustainability Evaluation," *ACS Environmental.Au,* vol. 2, no. 2, pp. 98-114, 2022.

[32] P. L. Ngo, I. A. Udugama, K. V. Gernaey and B. R. Young, "Mechanisms, status, and challenges of thermal hydrolysis and advanced thermal hydrolysis processes in sewage sludge treatment," *Chemosphere,* vol. 281, October 2021.

[33] S. Rasi, P. Kilpeläinen, K. Rasa, R. I. Korpinen, J.-E. Raitanen, M. Vainio, V. Kitunen, H. Pulkkinen and T. Jyske, "Cascade processing of softwood bark with hot water extraction, pyrolysis and anaerobic digestion," *Bioresource Technology,* July 2019.

[34] D. Fabbri and C. Torri, "Linking pyrolysis and anaerobic digestion (Py-AD) for the conversion of lignocellulosic biomass," *Current Opinion in Biotechnology,* vol. 38, pp. 167-173, April 2016.

[35] C. Z. Zaman, K. Pal, W. A. Yehye, S. Sagadevan, S. T. Shah, G. A. Adebisi, E. Marliana, R. F. Rafique and R. B. Johan, Pyrolysis: A Sustainable Way to Generate Energy from Waste, Intechopen, 2017.

[36] A. Bridgwater, "Review of fast pyrolysis of biomass and product upgrading," *Biomass and Bioenergy,* vol. 38, pp. 68-94, March 2012.

[37] N. Ghimire, R. Bakke and W. H. Bergland, "Liquefaction of lignocellulosic biomass for methane production: A review," *Bioresource Technology,* vol. 332, July 2021.

[38] G. Charis, G. Danha, E. Muzenda and T. Nhubu, "Modeling a Sustainable, Self-Energized Pine Dust Pyrolysis System With Staged Condensation for Optimal Recovery of Bio-Oil," *Frontiers in Energy Research,* February 2021.

[39] S. Seyedi, "Overcoming Anaerobic Digestion Toxicity of Aqueous Liquid from Wastewater Solids Pyrolysis," 2020.

[40] M. MartínMartín, "Chapter 5 - Syngas," pp. 199-297, 2016.

[41] D. H. Tay, R. T. Ng and D. K. Ng, "Modular Optimization Approach for Process Synthesis and Integration of an Integrated Biorefinery," *Computer Aided Chemical Engineering,* vol. 31, pp. 1045-1049, 2012.

[42] C. Z. Zaman, K. Pal, W. A. Yehye, S. Sagadevan, S. T. Shah, G. A. Ganiyu Abimbola Adebisi, E. Marliana, R. F. Rafique and R. B. Johan, Pyrolysis: A Sustainable Way to Generate Energy from Waste in Pyrolysis, London: IntechOpen, 2017.

[43] Q. Feng and Y. Lin, "Integrated processes of anaerobic digestion and pyrolysis for higher bioenergy recovery from lignocellulosic biomass: A brief review," *Renewable and Sustainable Energy Reviews,* vol. 77, pp. 1272-1287, September 2017.

[44] X.-D. Song, D.-Z. Chen, J. Zhang, X.-H. Dai and Y.-Y. Qi, "Anaerobic digestion combined pyrolysis for paper mill sludge disposal and its influence on char characteristics," *J Mater Cycles Waste Manag,* August 2015.

[45] A. S. Giwa, H. Xu, F. Chang, X. Zhang, N. Ali, J. Yuan and K. Wang, "Pyrolysis coupled anaerobic digestion process for food waste and recalcitrant residues: Fundamentals, challenges, and considerations," *Energy Science and Engineering,* October 2019.

[46] S. Tayibi, F. Monlau, F. Marias, G. Cazaudehore, N.-E. Fayoud, A. Oukarroum, Y. Zeroual and A. Barakat, "Coupling anaerobic digestion and pyrolysis processes for maximizing energy recovery and soil preservation according to the circular economy concept," *Journal of Environmental Management,* vol. 279, February 2021.

[47] S. Seyedi, K. Venkiteshwaran, N. Benn and D. Zitomer, "Inhibition during Anaerobic Co-Digestion of Aqueous Pyrolysis Liquid from Wastewater Solids and Synthetic Primary Sludge," *Sustainability,* April 2020.

[48] A. Mohammadi, G. Venkatesh, M. Sandberg, S. Eskandari and K. Granström, "Life cycle assessment of combination of anaerobic digestion and pyrolysis: focusing on different options for biogas use," *Advances in Geosciences,* p. 57–66, August 2019.

[49] M. Inyang, B. Gao, P. Pullammanappallil, W. Din and A. R. Zimmerman, "Biochar from anaerobically digested sugarcane bagasse," *Bioresource Technology,* vol. 101, no. 22, pp. 8868-8872, November 2010.

[50] C. A. Salman, S. Schwede, E. Thorin and J. Yan, "Predictive modelling and simulation of integrated pyrolysis and anaerobic digestion process," *Energy Procedia,* vol. 105, pp. 850-857, MAy 2017.

[51] C. AwaisSalman, S. Schwede, M. Naqvi, E. Thorin and J. Yan, "Synergistic combination of pyrolysis, anaerobic digestion, and CHP plants.," *Energy Procedia,* vol. 158, pp. 1323-1329, February 2019.

[52] H. Ozgun, "Anaerobic Digestion Model No. 1 (ADM1) for mathematical modeling of full-scale sludge digester performance in a municipal wastewater treatment plant," *Biodegradation,* p. 27–36, October 2018.

[53] D. Batstone, J. Keller, I. Angelidaki, S. Kalyuzhnyi, S. Pavlostathis,, A. Rozzi, W. Sanders, H. Siegrist and V. Vavilin, "The IWA Anaerobic Digestion Model No 1 (ADM1)," *Water Science & Technology,* p. 65–73, 2002.

[54] P. Das, C. V.P, T. Mathimani and A. Pugazhendhi, "A comprehensive review on the factors affecting thermochemical conversion efficiency of algal biomass to energy," *Science of The Total Environment,* vol. 766, April 2021.

[55] F. Monlau, C. Sambusiti, N. Antoniou and A. Barakat, "A new concept for enhancing energy recovery from agricultural residues by coupling anaerobic digestion and pyrolysis process," *Applied Energy,* vol. 148, pp. 32-38, 2015.

[56] F. Abnisa, A. Arami-Niya, W. M. A. Wan Daud and J. N. Sahu, "Characterization of Bio-oil and Bio-char from Pyrolysis of Palm Oil Wastes," *Bioenerg. Res,* p. 830–840, 2013.

[57] J. Brar, K. Tingi, J. Zondlo and J. Wang, "Co-Gasification of Coal and Hardwood Pellets: A Case Study," *Columbia International Publishing American Journal of Biomass and Bioenergy,* vol. 2, pp. 25-40, 2013.

[58] J. Chojnacki, J. Najser, K. Rokosz, V. Peer, J. Kielar and B. Berner, "Syngas Composition: Gasification of Wood Pellet with Water Steam through a Reactor with Continuous Biomass Feed System," *Energies,* vol. 13, no. 17, p. 4376, August 2020.

[59] M. Lübken, M. Wichern, M. Schlattmann, A. Gronauer and H. Horn, "Modelling the energy balance of an anaerobic digester fed with cattle manure and renewable energy crops," *Water Research,* vol. 41, no. 18, pp. 4085-4096, 2007.

[60] C. A.Wilson and J. T.Novak, "Hydrolysis of macromolecular components of primary and secondary wastewater sludge by thermal hydrolytic pretreatment," *Water Research,* vol. 43, pp. 4489-4498, October 2009.

[61] N. C. f. B. Information, "PubChem Compound Summary for CID 176, Acetic acid," 17 April 2022. [Online]. Available: https://pubchem.ncbi.nlm.nih.gov/compound/Acetic-acid..

[62] "National Center for Biotechnology Information. PubChem Compound Summary for CID 977, Oxygen," 17 April 2022. [Online]. Available: https://pubchem.ncbi.nlm.nih.gov/compound/Oxygen. [Accessed 17 April 2022].

[63] D. Raya, "Analysing Aqueous Pyrolysis Liquid as feed for Anaerobic Digestion," Porsgrunn, 2021.

[64] D. Orhon and E. Ubay Çokgör, "COD Fractionation in Wastewater Characterization—The State of the Art," *Journal of Chemical Technology & Biotechnology,* March 1999.

[65] P. Foladori, G. Andreottola and G. Ziglio, Sludge Reduction Technologies in Wastewater Treatment Plants, IWA Publishing, 2010, p. 380 .

[66] A. Akhiar, "Characterization of liquid fraction of digestates after solid-liquid separation from anaerobic co-digestion plants," 2017.

[67] G. Luo and I. Angelidaki, "Co-digestion of manure and whey for in situ biogas upgrading by the addition of H2: process performance and microbial insights," *Appl Microbiol Biotechnol,* p. 1373–1381, 2013.

[68] K. Shi, J. Yan, J. A. Menéndez, X. Luo, G. Yang, Y. Chen, E. Lester and T. Wu, "Production of H2-Rich Syngas From Lignocellulosic Biomass Using Microwave-Assisted Pyrolysis Coupled With Activated Carbon Enabled Reforming," *Frintiers in chemistry,* 2020.

[69] Y. Wang, L. Huang, T. Zhang and Q. Wang, "Hydrogen-rich syngas production from biomass pyrolysis and catalytic reforming using biochar-based catalysts," *Fuel,* vol. 313, 2022.

[70] S. Shah, "Methane from Syngas by Anaerobic Digestion," University of South Eastern Norway, Porsgrunn, 2016.

[71] R. Wahid, D. G. Mulat, J. C. Gaby and S. J. Horn, "Effects of H2:CO2 ratio and H2 supply fluctuation on methane content and microbial community composition during in-situ biological biogas upgrading," *Biotechnology for Biofuels and Bioproducts,* April 2019.

[72] G. Luo and I. Angelidaki, "Integrated biogas upgrading and hydrogen utilization in an anaerobic reactor containing enriched hydrogenotrophic methanogenic culture," *Biotechnology and bioengineering,* vol. 109, no. 11, 2729-2736.

[73] N. Mohajeri Nav, O. Prakash Bhujange, A. Ashim Aryal and P. Bakhtavar, "Pyrolysis products in industrial scale biogas reactor at Lindum," Porsgrunn, 2021.

Appendices

Appendix A Master's Thesis Description

Appendix B Mass Balance at Lindum

Appendix C Lab Calculations

Appendix D Effluent Data

Appendix E Biochemical rate coefficient and kinetic rate equation used in extended ADM1

Appendix A Master's Thesis Description

University of South-Eastern Norway

Faculty of Technology, Natural Sciences and Maritime Sciences, Campus Porsgrunn

FMH606 Master's Thesis

Title: Modelling heat treated lignocellulosic material as substrate in Anaerobic digestion

USN supervisor: Wenche Bergland

External partner: Gudny Øyre Flatabø at Scanship AS

Task background:
Energy and material production from lignocellulosic (wood) waste material receives increased interest as a carbon neutral economic feasible option. The master study will be carried out to gain more knowledge related to ongoing research projects in cooperation with industry. The projects aim at developing new technologies for converting various biomass waste products as lignocellulosic residue feedstocks into biogas (biomethane) transportation fuel and biocarbon material by combining anaerobic digestion (AD) and pyrolysis/gasification technology. Anaerobic digestion is a method where microorganisms mineralize organic matter, generating biogas. The biogas is an energy source due to its high content of methane. Understanding the mechanisms controlling the stoichiometry and kinetics in anaerobic digestion is important to improve the usage of heat-treated products of lignocellulosic components as lignin, hemicellulose and cellulose for transport fuel production (methane from upgraded biogas).

Task description:
The Anaerobic Digestion Model no 1 (ADM1) will be used as an analysing tool. It uses a range of standard model parameters but should also be adjusted based on the analyses in this case. The model should be evaluated using sludge/food waste fed full scale reactors at Lindum fed syngas from pyrolysis and Aqueous Pyrolysis Liquid (APL) as co-substrates in a continuous AD reactor. Topics to be addressed are effect of sludge/food waste organic loads, co-substrates, and co-digestion effects. The task includes:

- Literature review
- Analysis of relevant products from pyrolysis
- Analysis of anaerobic digestion mechanisms of pyrolysis products
- Adding digestion of APL and syngas to ADM1
- Simulation in ADM1

Student category: EET student (or other students that have completed the course EET2110)

Is the task suitable for online students (not present at the campus)? Yes

Practical arrangements:
-

Supervision:
As a general rule, the student is entitled to 15-20 hours of supervision. This includes necessary time for the supervisor to prepare for supervision meetings (reading material to be discussed, etc).

Signatures:

Supervisor (date and signature): 01.02.22 Wenche Bergland

Student (write clearly in all capitalized letters): ALIREZA RASTI

Student (date and signature): 01.02.2022

Appendix B Mass Balance at Lindum

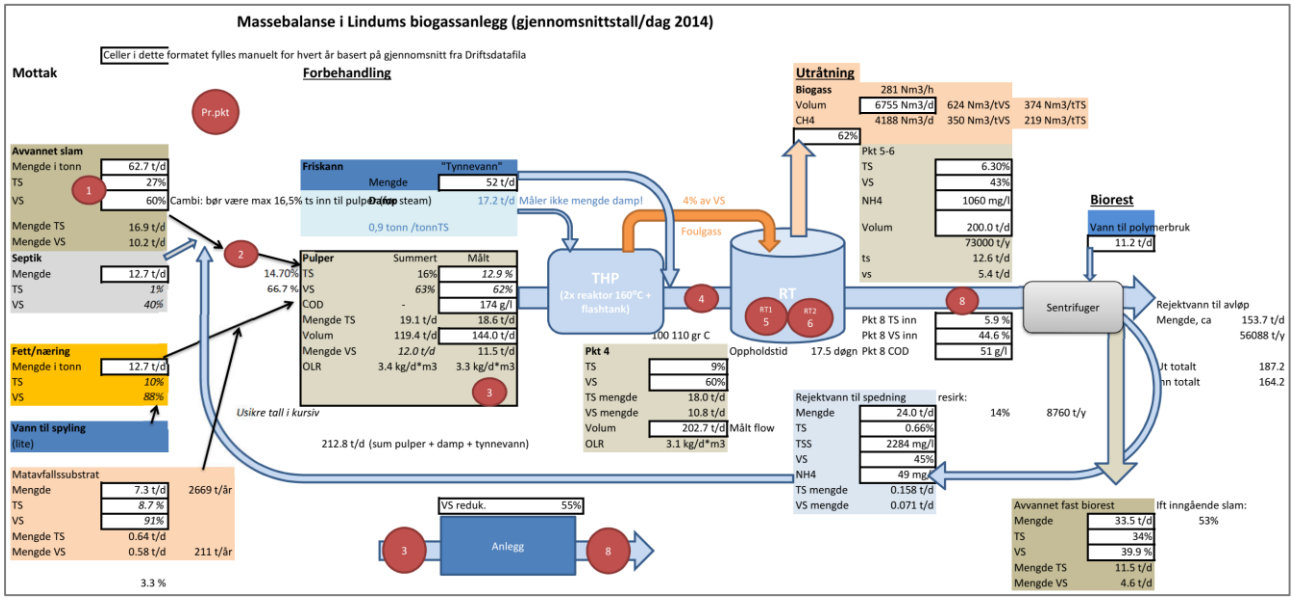

Appendix C Lab Calculations

Alkalinity				
Date	Sample	Dilution factor	Diluted Alkalinity (mg/L)	Real Alkalinity (mg/L)
16-Sep-21	Digestate	1:50	205.7	10285
16-Sep-21		1:50	202.6	10130
6-Oct-21		1:50	169.7	8485
6-Oct-21		1:50	169.9	8495
16-Sep-21	Hydrolyzed Sludge	2:100	109.8	5490
6-Oct-21		1:50	15.7	785
6-Oct-21		1:50	21.5	1075
29-Jul-21	APL	1:250	283.6	70900

Ammonium				
Date	Sample	Dilution factor	Diluted Ammonium (NH+4)(mg/L)	Real Ammonium (mg/L)
16-Sep-21	Digestate	1:50	52	2600
16-Sep-21		1:50	44.5	2225
24-Sep-21		1:50	50.7	2535
6-Oct-21		1:50	57.8	2890
6-Oct-21		1:50	57.3	2865
16-Sep-21	Hydrolyzed Sludge	2:100	33.8	1690
24-Sep-21		1:50	50.7	2535
6-Oct-21		1:50	17.8	890
6-Oct-21		1:50	17.6	880
29-Jul-21	APL	1:250	59.5	14875
16-Sep-21		1:500	32.3	16150

Appendix D Effluent Data

Effluent Gas Flow (m3/day)							
1	6019.727	92	8473.42	183	8342.556	274	10478.12
2	5862.916	93	8567.055	184	8239.896	275	9084.869
3	5752.359	94	8567.055	185	8428.295	276	8959.646
4	6063.724	95	8154.158	186	8635.871	277	7820.23
5	6081.774	96	9181.889	187	9032.975	278	7696.135
6	6202.485	97	9181.889	188	8444.088	279	7138.837
7	6377.346	98	8476.804	189	8112.417	280	9135.635
8	6002.805	99	8075.188	190	7792.027	281	8966.415
9	5640.674	100	8075.188	191	7567.528	282	8684.381
10	4987.484	101	7164.784	192	7902.584	283	10205.11
11	4435.826	102	7332.876	193	7863.099	284	9400.747
12	4337.678	103	6830.856	194	6533.028	285	9564.326
13	4276.759	104	6662.764	195	6220.535	286	9047.64
14	4811.495	105	6898.544	196	7063.252	287	8930.314
15	4811.495	106	7264.059	197	7282.11	288	4480.951
16	4929.949	107	6662.764	198	8034.576	289	4141.383
17	5116.091	108	6941.413	199	8062.779	290	6275.813
18	5129.629	109	7116.274	200	8234.255	291	8207.18
19	5129.629	110	6379.602	201	8310.969	292	8407.988
20	4413.263	111	6176.538	202	7665.675	293	8097.751
21	5376.69	112	6395.396	203	7922.89	294	6791.371
22	5895.632	113	5180.395	204	9087.125	295	5930.604
23	6360.424	114	8027.807	205	7875.509	296	5840.353
24	6433.752	115	8262.459	206	7424.255	297	5803.125
25	6875.981	116	8609.924	207	7997.347	298	6203.613
26	7682.597	117	8609.924	208	8198.155	299	6246.482
27	7139.965	118	7085.814	209	7465.996	300	5877.582
28	6544.31	119	8743.044	210	7652.138	301	6306.273
29	5798.612	120	9020.565	211	8039.088	302	6540.925
30	7129.811	121	8515.161	212	8168.824	303	6837.625
31	7190.731	122	9065.691	213	7948.837	304	7651.01
32	7306.929	123	8360.606	214	6283.71	305	8034.576
33	7768.336	124	7796.539	215	5072.094	306	7689.366
34	7460.355	125	8051.498	216	5982.498	307	7766.079
35	7558.503	126	8669.715	217	7119.658	308	8034.576
36	7558.503	127	8410.244	218	7788.642	309	7705.16

37	7445.689	128	8724.994	219	7986.066	310	6534.156
38	7353.182	129	9267.627	220	8915.649	311	6887.262
39	7861.971	130	9591.401	221	6684.198	312	6756.399
40	8351.581	131	9310.496	222	7016.998	313	5736.565
41	7564.143	132	8658.434	223	7610.397	314	6651.482
42	7094.839	133	3366.354	224	7850.69	315	8198.155
43	7094.839	134	4896.105	225	8101.135	316	7718.698
44	6917.722	135	6908.697	226	7890.174	317	8086.47
45	6836.496	136	8146.261	227	8188.002	318	7746.901
46	6836.496	137	7259.547	228	8602.027	319	7792.027
47	6423.599	138	6766.552	229	8952.877	320	7886.79
48	5868.557	139	8244.409	230	8200.411	321	7468.252
49	6363.808	140	8784.785	231	8781.401	322	8226.358
50	5267.261	141	8198.155	232	8702.431	323	8180.105
51	5435.353	142	8366.247	233	8285.021	324	7046.329
52	5587.651	143	9096.15	234	9003.643	325	6107.721
53	5800.869	144	7855.202	235	7831.511	326	6826.343
54	6450.674	145	8939.34	236	7928.531	327	6966.232
55	5956.551	146	7102.736	237	8523.058	328	6403.293
56	6416.83	147	7243.753	238	8872.78	329	4504.642
57	6759.783	148	5639.545	239	9233.783	330	4730.269
58	6000.549	149	6273.557	240	8451.985	331	5102.553
59	5607.958	150	6839.881	241	8837.807	332	5245.826
60	6156.231	151	7473.893	242	8450.857	333	6148.334
61	6148.334	152	7878.893	243	9780.928	334	6742.861
62	6651.482	153	8363.991	244	9606.067	335	7167.04
63	7508.865	154	8437.32	245	9140.148	336	7766.079
64	8246.665	155	9117.585	246	8453.113	337	8444.088
65	8246.665	156	9203.323	247	8502.751	338	9423.309
66	7831.511	157	9125.482	248	8620.077	339	8603.155
67	8093.239	158	8697.919	249	7557.375	340	7592.347
68	7658.907	159	8652.793	250	7849.561	341	7108.377
69	5937.373	160	8511.776	251	8129.339	342	7651.01
70	6643.585	161	7817.974	252	9208.964	343	7603.628
71	8174.464	162	7669.06	253	9501.151	344	7010.229
72	8954.005	163	7362.207	254	6275.813	345	7079.045
73	6919.978	164	8501.623	255	8485.829	346	8906.624
74	6196.844	165	8351.581	256	8638.128	347	9806.875
75	6996.692	166	7714.185	257	8230.871	348	8817.501

76	7983.809	167	7975.913	258	8067.291	349	9114.2
77	7169.296	168	7409.589	259	8990.106	350	9001.387
78	6693.223	169	7758.183	260	9576.736	351	9444.744
79	6107.721	170	7400.564	261	9555.301	352	8688.894
80	6237.457	171	8112.417	262	9520.329	353	7452.458
81	6237.457	172	8431.679	263	9597.042	354	10245.72
82	4984.099	173	8121.442	264	9802.363	355	10104.7
83	4993.124	174	7770.592	265	9982.864	356	10297.61
84	5868.557	175	7949.965	266	9141.276	357	9826.053
85	7027.151	176	8362.863	267	10818.81	358	8323.378
86	8173.336	177	8392.194	268	10932.75	359	8327.891
87	8713.713	178	7815.717	269	10049.42	360	8222.974
88	8712.584	179	7688.238	270	10574.01	361	8026.679
89	8252.306	180	8800.579	271	9946.764	362	7209.909
90	8396.707	181	9106.303	272	10220.9	363	6859.059
91	8473.42	182	7943.197	273	10227.67	364	7604.756
						365	7726.595

Effluent Methane Percentage									
2	61.00058	81	55.99928	178	62.70064	287	63	337	64.6
6	61.20044	84	61.2995	185	63.80003	290	64.1	342	62.7
9	56.9	92	62.50033	186	64.50033	293	62.7	346	63.2
10	57.90093	95	64.09934	192	63.40043	294	60.9	352	64.1
13	57.00079	98	62.99973	195	64.90025	295	61	363	63.8
14	61.09965	101	61.99969	198	64.19966	296	62.2		
15	61.09965	104	63.00034	202	64.4	297	60.2		
16	61.29977	105	62.79967	205	63.6	300	60.1		
22	62.60046	114	62.79933	213	64.5	301	59.8		
24	63.99965	118	62.99952	220	63.4	302	60.3		
25	66.90074	119	62.30065	227	63.9	303	63.2		
34	63.60048	125	63.79992	231	64	304	62.7		
37	63	129	62.5003	233	64.1	307	61.4		
43	62.20067	132	64.50033	241	64.1	311	61		
44	62.5	136	62.20053	246	63.8	314	61.9		
48	61.69935	139	63.60016	248	63.9	317	61.4		
51	59.80075	142	62.69957	252	63.9	318	60		
59	61.29954	153	63.69976	255	64.5	323	61.6		
63	61.40024	154	63.50047	262	63.2	325	60.5		

65	61.70041	157	63.39968	265	64.2	330	58.2		
66	62.19965	164	63.39968	269	63.7	331	58.6		
70	62.20071	171	63.09971	276	63.6	332	58.2		
73	62.39974	174	64.20006	282	63.7	334	60.2		
79	61.49982	176	63.29961	283	63.6	335	65.2		

Effluent CO2 Percentage							
13	42.99921	119	37.69935	252	36.1	334	39.8
14	38.90035	125	36.20008	255	35.5	335	34.8
15	38.90035	129	37.4997	262	36.8	337	35.4
16	38.70023	132	35.49967	265	35.8	342	37.3
22	37.39954	136	37.79947	269	36.3	346	36.8
24	36.00035	139	36.39984	276	36.4	352	35.9
25	33.09926	142	37.30043	282	36.3	363	36.2
34	36.39952	153	36.30024	283	36.4		
37	37	154	36.49953	287	37		
43	37.79933	157	36.60032	290	35.9		
44	37.5	164	36.60032	293	37.3		
48	38.30065	171	36.90029	294	39.1		
51	40.19925	174	35.79994	295	39		
59	38.70046	176	36.70039	296	37.8		
63	38.59976	178	37.29936	297	39.8		
65	38.29959	185	36.19997	300	39.9		
66	37.80035	186	35.49967	301	40.2		
70	37.79929	192	36.59957	302	39.7		
73	37.60026	195	35.09975	303	36.8		
79	38.50018	198	35.80034	304	37.3		
81	44.00072	202	35.6	307	38.6		
84	38.7005	205	36.4	311	39		
92	37.49967	213	35.5	314	38.1		
95	35.90066	220	36.6	317	38.6		
98	37.00027	227	36.1	318	40		
101	38.00031	231	36	323	38.4		
104	36.99966	233	35.9	325	39.5		
105	37.20033	241	35.9	330	41.8		
114	37.20067	246	36.2	331	41.4		
118	37.00048	248	36.1	332	41.8		

Appendix E Biochemical rate coefficient and kinetic rate equation used in extended ADM1

j	Component → / Process ↓	i	1 S_{su}	2 S_{aa}	3 S_{fa}	4 S_{va}	5 S_{bu}	6 S_{pro}	7 S_{ac}	8 S_{h2}	9 S_{ch4}	10 S_{IC}	11 S_{IN}	12 S_{I}	Rate (ρ_j, kg COD.m^{-3}.d^{-1})
1	Disintegration													$f_{sI,xc}$	$k_{dis}X_c$
2	Hydrolysis carbohydrates		1												$k_{hyd,ch}X_{ch}$
3	Hydrolysis of proteins			1											$k_{hyd,pr}X_{pr}$
4	Hydrolysis of lipids		$1-f_{fa,li}$		$1-f_{fa,li}$										$k_{hyd,li}X_{li}$
5	Uptake of sugars		−1				$(1-Y_{su})f_{bu,su}$	$(1-Y_{su})f_{pro,su}$	$(1-Y_{su})f_{ac,su}$	$(1-Y_{su})f_{h2,su}$		$-\sum_{i=9,11\text{-}24} C_i v_{i,5}$	$-(Y_{su})\,N_{bac}$		$k_{m,su}\frac{S_{su}}{K_S+S}X_{su}I_1$
6	Uptake of amino acids			−1		$(1-Y_{aa})f_{va,aa}$	$(1-Y_{aa})f_{bu,aa}$	$(1-Y_{aa})f_{pro,aa}$	$(1-Y_{aa})f_{ac,aa}$	$(1-Y_{aa})f_{h2,aa}$		$-\sum_{i=1\text{-}9,11\text{-}24} C_i v_{i,6}$	$N_{aa}-(Y_{aa})\,N_{bac}$		$k_{m,aa}\frac{S_{aa}}{K_S+S_{aa}}X_{aa}I_1$
7	Uptake of LCFA				−1				$(1-Y_{fa})\,0.7$	$(1-Y_{fa})\,0.3$			$-(Y_{fa})\,N_{bac}$		$k_{m,fa}\frac{S_{fa}}{K_S+S_{fa}}X_{fa}I_2$
8	Uptake of valerate					−1		$(1-Y_{c4})\,0.54$	$(1-Y_{c4})\,0.31$	$(1-Y_{c4})\,0.15$			$-(Y_{c4})\,N_{bac}$		$k_{m,c4}\frac{S_{su}}{K_S+S_{su}}X_{c4}\frac{1}{1+S_{bu}/S_{su}}I$
9	Uptake of butyrate						−1		$(1-Y_{c4})\,0.8$	$(1-Y_{c4})\,0.2$			$-(Y_{c4})\,N_{bac}$		$k_{m,c4}\frac{S_{su}}{K_S+S_{su}}X_{c4}\frac{1}{1+S_{bu}/S_{su}}I$
10	Uptake of propionate							−1	$(1-Y_{pro})\,0.57$	$(1-Y_{pro})\,0.43$		$-\sum_{i=1\text{-}9,11\text{-}24} C_i v_{i,10}$	$-(Y_{pro})\,N_{bac}$		$k_{m,pro}\frac{S_{su}}{K_S+S_{pro}}X_{pro}I_3$
11	Uptake of acetate								−1		$(1-Y_{ac})$	$-\sum_{i=1\text{-}9,11\text{-}24} C_i v_{i,11}$	$-(Y_{ac})\,N_{bac}$		$k_{m,ac}\frac{S_{ac}}{K_S+S_{ac}}X_{ac}I_3$
12	Uptake of hydrogen									−1	$(1-Y_{h2})$	$-\sum_{i=1\text{-}9,11\text{-}24} C_i v_{i,12}$	$-(Y_{h2})\,N_{bac}$		$k_{m,h2}\frac{S_{h2}}{K_S+S_{h2}}X_{h2}I_1$
13	Decay of X_{su}														$k_{dec,Xsu}X_{su}$
14	Decay of X_{aa}														$k_{dec,Xaa}X_{aa}$
15	Decay of X_{fa}														$k_{dec,Xfa}X_{fa}$
16	Decay of X_{c4}														$k_{dec,Xc4}X_{c4}$
17	Decay of X_{pro}														$k_{dec,Xpro}X_{pro}$
18	Decay of X_{ac}														$k_{dec,Xac}X_{ac}$
19	Decay of X_{h2}														$k_{dec,Xh2}X_{h2}$
			Monosaccharides (kgCOD.m^{-3})	Amino acids (kgCOD.m^{-3})	Long chain fatty acids (kgCOD.m^{-3})	Total valerate (kgCOD.m^{-3})	Total butyrate (kgCOD.m^{-3})	Total propionate (kgCOD.m^{-3})	Total acetate (kgCOD.m^{-3})	Hydrogen gas (kgCOD.m^{-3})	Methane gas (kgCOD.m^{-3})	Inorganic carbon (kmoleC.m^{-3})	Inorganic nitrogen (kmoleN.m^{-3})	Soluble inerts (kgCOD.m^{-3})	Inhibition factors: $I_1=I_{pH}I_{IN,lim}$ $I_2=I_{pH}I_{IN,lim}I_{h2}$ $I_3=I_{pH}I_{IN,lim}I_{hh3,Xac}$

j	Component → / Process ↓	i	13 X_c	14 X_{ch}	15 X_{pr}	16 X_{li}	17 X_{su}	18 X_{aa}	19 X_{fa}	20 X_{c4}	21 X_{pro}	22 X_{ac}	23 X_{h2}	24 X_{I}	Rate (ρ_j, kg COD.m^{-3}.d^{-1})
1	Disintegration		-1	$f_{ch,xc}$	$f_{pr,xc}$	$f_{li,xc}$								$f_{xI,xc}$	$k_{dis}X_c$
2	Hydrolysis carbohydrates			-1											$k_{hyd,ch}X_{ch}$
3	Hydrolysis of proteins				-1										$k_{hyd,pr}X_{pr}$
4	Hydrolysis of lipids					-1									$k_{hyd,li}X_{li}$
5	Uptake of sugars						Y_{su}								$k_{m,su}\frac{S_{su}}{K_S+S}X_{su}I_1$
6	Uptake of amino acids							Y_{aa}							$k_{m,aa}\frac{S_{aa}}{K_S+S_{aa}}X_{aa}I_1$
7	Uptake of LCFA								Y_{fa}						$k_{m,fa}\frac{S_{fa}}{K_S+S_{fa}}X_{fa}I_2$
8	Uptake of valerate									Y_{c4}					$k_{m,c4}\frac{S_{su}}{K_S+S_{su}}X_{c4}\frac{1}{1+S_{bu}/S_{su}}I$
9	Uptake of butyrate									Y_{c4}					$k_{m,c4}\frac{S_{su}}{K_S+S_{su}}X_{c4}\frac{1}{1+S_{bu}/S_{su}}I$
10	Uptake of propionate										Y_{pro}				$k_{m,pro}\frac{S_{su}}{K_S+S_{pro}}X_{pro}I_3$
11	Uptake of acetate											Y_{ac}			$k_{m,ac}\frac{S_{ac}}{K_S+S_{ac}}X_{ac}I_3$
12	Uptake of hydrogen												Y_{h2}		$k_{m,h2}\frac{S_{h2}}{K_S+S_{h2}}X_{h2}I_1$
13	Decay of X_{su}		1				-1								$k_{dec,Xsu}X_{su}$
14	Decay of X_{aa}		1					-1							$k_{dec,Xaa}X_{aa}$
15	Decay of X_{fa}		1						-1						$k_{dec,Xfa}X_{fa}$
16	Decay of X_{c4}		1							-1					$k_{dec,Xc4}X_{c4}$
17	Decay of X_{pro}		1								-1				$k_{dec,Xpro}X_{pro}$
18	Decay of X_{ac}		1									-1			$k_{dec,Xac}X_{ac}$
19	Decay of X_{h2}		1										-1		$k_{dec,Xh2}X_{h2}$
			Composites (kgCOD.m^{-3})	Carbohydrates (kgCOD.m^{-3})	Proteins (kgCOD.m^{-3})	Lipids (kgCOD.m^{-3})	Sugar degraders (kgCOD.m^{-3})	Amino acid degraders (kgCOD.m^{-3})	LCFA degraders (kgCOD.m^{-3})	Valerate and butyrate degraders (kgCOD.m^{-3})	Propionate degraders (kgCOD.m^{-3})	Acetate degraders (kgCOD.m^{-3})	Hydrogen degraders (kgCOD.m^{-3})	Particulate inerts (kgCOD.m^{-3})	Inhibition factors: $I_1=I_{pH}I_{IN,lim}$ $I_2=I_{pH}I_{IN,lim}I_{h2}$ $I_3=I_{pH}I_{IN,lim}I_{hh3,Xac}$